

Atmosphere

Volume 12 Number 1 1974

Canadian Meteorological Society
Société Météorologique du Canada

Atmosphere

Volume 12 Number 1 1974

Contents

1

Editorial

Note from the Executive

2

A Synoptic Parameterization of the Drag Coefficient

Joan Vyverberg Jensen

9

Révérénd Père Ernesto Gherzi 1886-1973

10

The Use of Isentropic Coordinates in the Formulation
of Objective Analysis and Numerical Prediction Models

M.A. Shapiro

18

An Operational Windchill Index

H.T. Beal

31

The Correlation of Snowpack with Topography and Snowmelt
Runoff on Marmot Creek Basin, Alberta

Douglas L. Golding

39

Book Review

40

Advertisement

EDITORIAL

It is now eleven years since the founding of *Atmosphere*. In that time it has served as the official publication of first the Canadian Branch of the Royal Meteorological Society and, since 1967, the Canadian Meteorological Society. As such it has had to play many roles including that of news bulletin for the Society as well as carrier of articles of general interest to the members. Beginning in 1971 *Atmosphere* appeared in its present physical format and at about the same time began to increase the percentage of its content devoted to research articles. With the establishment in 1973 of a Newsletter distributed to all members the way would now seem to be open to pursue in earnest the conversion of *Atmosphere* into a full-fledged research journal. That is the aim of Council and of the new editorial committee and it is the reason for this editorial.

In order to inform prospective authors, a statement of Editorial Policy will appear on the inside back cover of *Atmosphere*, starting with this issue. Although we hope eventually to obtain submissions from the international scientific community we shall have to depend at first mainly on contributions from members of the CMS. If we can obtain papers of a sufficiently high scientific standard the success of the journal will be automatically ensured. This will require a certain amount of faith on the part of early contributors who are being asked to publish their best work in a journal of limited readership. Many have already shown that faith. The Editorial Committee fervently hopes that more will do so.

NOTE FROM THE EXECUTIVE

At an executive meeting held on 18 December, 1973 it was moved by the President, seconded by the Vice-President and unanimously resolved by the Executive Committee on behalf of the CMS to acknowledge the great contributions made to the development of *Atmosphere* by E.J. Truhlar. When Mr. Truhlar retires from the editorship with the appearance in early 1974 of Volume 11, No. 4 (the Andrew Thomson Anniversary Issue) he will have edited sixteen issues, extending over four eventful years during which our journal has been making a transition from a news bulletin of the Society to a respected Canadian vehicle for the dissemination of meteorological science. During this period, *Atmosphere* was the principal tie of the Society, and Mr. Truhlar's devotion and leadership are noted with appreciation.

A Synoptic Parameterization of the Drag Coefficient

Joan Vyverberg Jensen

*Department of Mechanical Engineering
University of Waterloo, Waterloo, Ontario*

[Manuscript received 18 November 1973; in revised form 7 January 1974]

ABSTRACT

The frictional force exerted on the atmosphere over Lake Erie is investigated by incorporating synoptic weather data into boundary layer theory. Over-water data obtained during a severe winter storm by the CCGS N.B. McLean on Lake Erie are used.

The friction force is a function of the drag coefficient C_d . The following expression for C_d is developed which depends primarily on synoptic data: $C_d = f|\vec{V}_g| h V^{-2} \sin \delta$, where δ is the angle between \vec{V} and \vec{V}_g . Drag coefficients were calculated using values of the boundary layer depth h which were

determined from constructed temperature profiles. This depth varies considerably with stability. Approximate values are $h = 0.1$ km for stable, 1 km for neutral, and 1.8 km for unstable conditions.

Drag coefficients over water for unstable conditions appear to be two to ten times larger than for stable circumstances, and are up to eight times the value suggested by Cressman (1960). C_d also varies according to whether it is computed for an over-water, an up-wind or a downwind location.

1 Introduction

Non-adiabatic and windy conditions often prevail during mid-latitude winter storms. The incorporation of these characteristics into numerical prognoses is being studied at the University of Waterloo (Danard, 1971). Frictionally-induced fluxes of sensible heat and water vapour are included in the numerical model as *spatially varying* quantities (Danard and Rao, 1972). The influence of large water bodies is felt through these fluxes, which in turn are dependent on the drag coefficient. These energy flux terms make especially large contributions to the deepening of a storm in locales where a cold air mass comes in contact with a warm body of water. Is the standard value of the drag coefficient for water surfaces, as determined by Cressman (1960), suitable for this situation?

The present study utilizes data obtained on Lake Erie and from surrounding weather stations during the 25–27 January 1971 storm, which was especially severe in the Southern Ontario–Central New York area. These synoptic weather observations are incorporated with boundary layer theory to develop an expression for calculating the drag coefficient. The next section discusses this derivation. The following sections are concerned with the data used and analyses per-

formed, the influence of stability on the boundary layer thickness, and the drag coefficients obtained.

2 Derivation of expression for drag coefficient

The equation governing atmospheric motion can be expressed as

$$\frac{d\vec{V}}{dt} = -\alpha\nabla_H P - f\vec{k} \times \vec{V} + \vec{F} \quad (1)$$

where $d\vec{V}/dt$ is the acceleration of the air parcel, $-\alpha\nabla_H P$ is the horizontal pressure force, $-f\vec{k} \times \vec{V}$ is the Coriolis force and \vec{F} is the friction force, all forces per unit mass. Surface trajectory calculations show that the acceleration term, especially for over-water locations, is small compared with other terms in Eq. (1) and can be ignored. The friction force then balances the pressure and Coriolis forces and must be included in numerical prognoses of storm system development.

Let $\vec{F} = -F\vec{i}$, where \vec{i} is the unit vector directed along the observed surface wind (at 10m); the frictional force is assumed to act oppositely to the surface wind. The magnitude of the friction force may be written

$$F = -\alpha|\nabla_H P| \sin \delta \quad (2)$$

$$F = f|\vec{V}_g| \sin \delta \quad (3)$$

where α is the specific volume, δ is the angle between the geostrophic (\vec{V}_g) and surface (\vec{V}) winds, and f is the Coriolis parameter.

The frictional force is often represented in boundary layer theory by

$$\vec{F} = \frac{1}{\rho} \frac{\partial \vec{\tau}}{\partial z} \quad (4)$$

where $\vec{\tau}$ is the horizontal stress which is assumed to vary linearly with height in the frictional boundary layer. In finite difference form Eq. (4) becomes

$$\vec{F} = \frac{1}{\rho} \frac{\vec{\tau}_h - \vec{\tau}_0}{h} \quad (5)$$

where h is chosen to be the height where the shearing stress due to surface friction becomes negligible, and $z = 0$ for $\vec{\tau}_0$. The surface stress $\vec{\tau}_0$ has the empirically determined form

$$\vec{\tau}_0 = -\rho C_d V^2 \vec{i} \quad (6)$$

where C_d represents the drag coefficient at the height of the observed surface wind.

Setting $\vec{\tau}_h = 0$, combining (5) and (6), and using (3), gives

$$C_d = \frac{f|\vec{V}_g|h \sin \delta}{V^2}. \quad (7)$$

Expression (7) represents the drag coefficient at $z = 10$ m. The assumptions made in deriving this formula imply a simple model of the wind stress caused

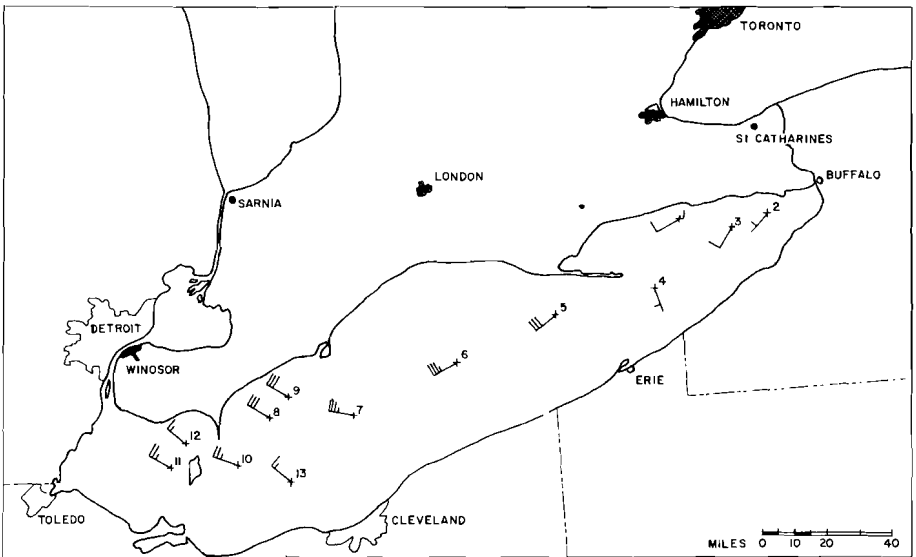


Fig. 1 Location of cgs N.B. McLean on Lake Erie at observation times. Numbers indicate successive positions. Wind speeds shown by full (10 m sec^{-1}) and half (5 m sec^{-1}) barbs.

by friction near the earth's surface. However, Eq. (7) is identical, save for the absence of the thermal wind term, to the "angle equation" of Venkatesh and Csanady (1973). The latter equation is based on a more sophisticated model than that employed in this paper; therefore the similarity of the two equations is encouraging.

3 Initial data and analyses performed

The low-pressure system associated with the storm of 25–27 January 1971 originated east of the Montana Rockies; when over Wisconsin it rapidly developed into an intense winter storm, bringing gale-force winds and heavy drifting to the Lake Erie region and up to 40 cm of snow in the London, Ontario, area (see Fig. 1). During this time, the ice-breaker cgs N.B. McLean was cruising on Lake Erie taking weather observations. The successive locations of the ship are plotted in Fig. 1, as well as the winds observed.

Information from the hourly teletype networks surrounding the Great Lakes was used in conjunction with the ship reports to draw separate streamline and pressure analyses. After the two independent analyses were completed, the maps for each time period were superimposed and the angle δ between the streamlines and isobars was determined for each point where a drag coefficient calculation would be made. The geostrophic wind at that point was also calculated.

Drag coefficients for the N.B. McLean and for near-shoreline locations upwind and downwind of Lake Erie (see Appendix) could then be determined. As a first approximation in these computations, h (the depth of the friction

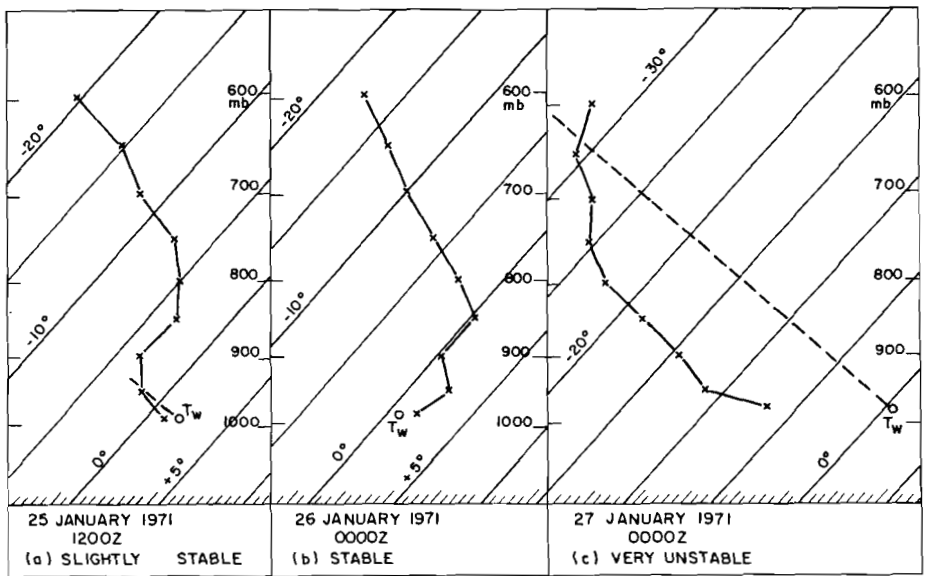


Fig. 2 Temperature soundings constructed for N.B. McLean plotted on tephigram for (a) slightly stable, (b) stable, and (c) very unstable conditions. Temperatures are in degrees Centigrade. Dashed lines in (a) and (c) indicate dry adiabats. Note water temperature (T_w) observed by N.B. McLean compared to surface air temperature (lowest x).

layer) was assumed to equal 1 km in accordance with previous boundary layer studies. However, most theoretical representations of the boundary layer are based on conditions of neutral stability. Therefore an empirical parameterization of the stability in terms of h was developed which could be used in Eq. (7) for the observed non-neutral conditions.

This was done by plotting the upper air temperatures observed at 50 mb intervals (from 950 to 600 mb) by the six radiosonde stations nearest to Lake Erie (SSM, GRB, FNT, PIT, DAY, BUF). The horizontal field was then drawn for each level and temperatures were interpolated for the location of the McLean and of the upwind and downwind stations. These values and the surface air temperature (also water temperature for the McLean) were plotted on a tephigram, giving a reconstructed vertical profile above each point.

Thus three temperature profiles were available for each time. These reconstructed soundings generally gave a clear visual indication of the top of the mixed layer. Specifically, this limit was taken to be the level closest to the earth's surface where the rate of increase of potential temperature became greater than approximately 5°C per 50 mb. For example, in Fig. 2(a) this occurs at 900 mb, in Fig. 2(b) at 985 mb (the surface), in Fig. 2(c) at 650 mb.

4 Influence of stability on boundary layer thickness

Table 1 shows the median values of the boundary layer depth (in km) obtained. The medians include data from the three locations, but are segregated accord-

TABLE 1. Median and range of boundary layer depths.

	Median (km)	Range (km)
Stable	0.1 (estimated)	0.10-0.14
Neutral	0.9	0.87-0.91
Very unstable	1.8	1.63-1.90

TABLE 2. Drag coefficient (C_d) and top of friction layer (h) for land and water locations. Stability categories are: stable (s), neutral (n), unstable (u).

Time	Location	Stability ¹	C_d ($\times 10^{-3}$)	h (km)
12z 25 Jan	Upwind (ERI)	N	31.8	0.90
	McLean	N	3.93	0.91
	Downwind (BUF)	N	2.67	0.87
00z 26 Jan	Upwind (ERI)	s	0.162	0.1 ²
	McLean	s	1.02	0.1 ²
	Downwind (MK)	s	0.236	0.1 ²
12z 26 Jan	Upwind (TOL)	U	39.4	1.63
	McLean	s	0.092	0.14
	Downwind (MK)	s	1.45	0.13
00z 27 Jan	Upwind (DTW)	U	25.1	1.80
	McLean	U	6.15	1.80
	Downwind (CLE)	U	30.6	1.80
12z 27 Jan	Upwind (DTW)	U	29.5	1.90
	McLean	U	4.12	1.89
	Downwind (CLE)	U	125.	1.90

¹McLean stability determined by T_{air} , T_{water} and $\partial\theta/\partial z$ on tephigram; others determined by $\partial\theta/\partial z$ only.

²Entire lower atmosphere was stable. $h = 0.1$ km assumed for sake of computation.

ing to observed low level stability. The range of the depths within each stability category is quite small, as shown in the last column. The small variability may be due to the lack of fine resolution inherent in the procedure used to construct the temperature profiles. However, the disparity between the medians for the *different* stability cases is large. These lake-storm data follow the same trend as the Wangara data (Venkatesh and Csanady, 1973), although here the ratio of unstable to stable values is much larger. Perhaps this is because extremely stormy conditions were prevalent over Lake Erie during the period of observation.

The boundary layer depths (h) determined from the constructed temperature profiles are shown in Table 2, as well as the drag coefficients (C_d) obtained. The strong dependence of h values on stability is particularly noticeable at 12Z 26 January when the upwind station was located in the unstable sector behind the cold front. The McLean and the downwind station were still in the warm stable air.

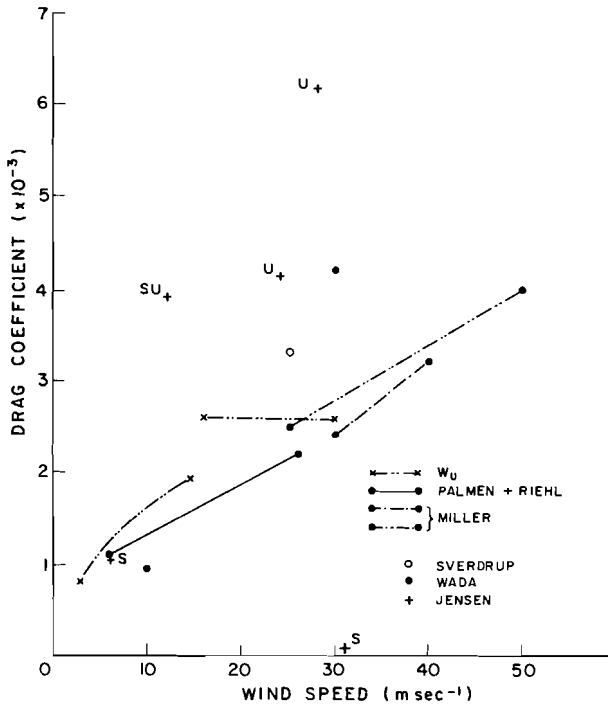


Fig. 3 Drag coefficients as a function of wind speed. Values are for studies conducted during high winds (after Wada, 1969). + indicates values computed in this study from McLean data during times of stable (s), neutral (su) and unstable (u) temperature profiles.

5 Computed drag coefficients

The suitability of the commonly accepted values of the drag coefficient in situations where high winds are observed is questionable. Fig. 3 shows C_d values obtained by Wada (1969) and summarizes her review of other studies which utilize wind velocities approaching typhoon magnitudes. Also on Fig. 3 are the five McLean drag coefficients computed in this study (+). For a given wind speed observed by the McLean, the “unstable” drag coefficients are many times larger than the “stable” values. Note that while individual points are plotted for the Sverdrup, Wada and Jensen studies, the data from other studies have been summarized by one or two lines. Therefore the scatter shown by the separate points is not necessarily inconsistent with results from the other studies. Additional data obtained at high wind speeds and non-neutral stabilities would be helpful in further defining the pattern emerging on Fig. 3.

Table 3 shows the median values for the drag coefficients in Table 2, separated by location and stability. The effect of instability is again very noticeable; however, the variation is opposite in sense to that which might be expected intuitively. This is being studied further.

Because of the small size of the data sample, the derived values of C_d should

TABLE 3. Medians of drag coefficients in Table 2.

Stability	Drag coefficient ($\times 10^{-3}$)		
	Upwind	McLean	Downwind
Stable	0.162	0.55	0.84
Unstable	29.5	5.13	77.8

only be viewed as indicating the order of magnitude. However, the data on Fig. 3 and the medians given in Table 3 imply that for unstable windy conditions the drag coefficient is much higher than the value of 1.2×10^{-3} normally used.

6 Conclusion

Heat and moisture exchanges at the air-earth interface are known to be greater during unstable conditions. Using a variable h when computing the drag coefficient emphasizes the effect of these exchanges. The destabilizing influence of the lakes on downwind locations is shown by the downwind drag coefficients, which are larger by a factor of three than the upwind values. Thus it appears that the exchange terms incorporating the drag coefficient should be adjusted according to land-water location and atmospheric stability. The wind velocity also appears to have a large influence, although extreme variability of wind speeds precludes any systematic categorization in this paper.

Acknowledgements

This research, conducted under the auspices of the Department of Mechanical Engineering, University of Waterloo, with the encouragement of Professor M.B. Danard, was supported by grants from the National Research Council of Canada and the Atmospheric Environment Service.

Preparation of the manuscript was greatly facilitated by Professor R.V. Jones, Department of Natural Philosophy, Aberdeen University, Scotland.

Appendix

Locations of Drag Coefficient Calculations.

Date/Time	McLean Locater Point	Upwind	Downwind
25 January 12z	1	ERI	BUF
26 January 00z	4	ERI	MK
26 January 12z	5	TOL	MK
27 January 00z	9	DTW	CLE
27 January 12z	10	DTW	CLE

References

- CRESSMAN, G.P., 1960: Improved terrain effects in barotropic forecasts. *Mon. Wea. Rev.*, **88**, 327-342.
- DANARD, M.B., 1971: A numerical study of the effects of long-wave radiation and surface friction on cyclone development. *Mon. Wea. Rev.*, **99**, 831-839.
- DANARD, M.B. and G.V. RAO, 1972: Numerical study of the effects of the Great Lakes on a winter cyclone. *Mon. Wea. Rev.*, **100**, 374-382.
- VENKATESH, S. and G.T. CSANADY, 1973: A planetary boundary layer model, and its application to the Wangara data. In press.
- WADA, M., 1969: Concerning the mechanism of the decaying of typhoon. *J. Met. Soc. Japan*, **47**, 335-351.
-

RÉVÉREND PÈRE ERNESTO GHERZI, S.J. 1886-1973

À Saint-Jérôme, près de Montréal, le 6 décembre 1973, est décédé, à l'âge de 87 ans et 4 mois, le Père Ernesto Gherzi, assigné depuis plus de 18 années à l'Observatoire de Géophysique du Collège Jean-de-Brébeuf.

Né à San-Remo, Italie, le 8 août 1886, il entra chez les jésuites le 22 octobre 1903, fit un premier séjour à Shanghai, Chine, de 1910 à 1913, fut ordonné prêtre en Angleterre le 29 juin, 1916, et repartit pour la Chine en octobre 1920, cette fois pour y entreprendre une longue carrière scientifique de près de trente années à l'Observatoire météorologique, sismique et magnétique de Zi Ka Wei, à Shanghai. Il y assumait des fonctions importantes dans les services radio pour la navigation, les signaux horaires et tout particulièrement dans la prévision du temps. Il y acquit une renommée proverbiale par sa façon de prédire et de suivre les typhons. Sur la seule météorologie et climatologie de Chine, il a publié plus de vingt volumes et plusieurs articles.

Expulsé de Chine en 1949 par les Communistes chinois, il demeura quelques mois à Hong Kong, puis fut appelé par les autorités portugaises pour réorganiser et compléter l'Observatoire de Macao. Il demeura quatre années à Macao, jusqu'à 1954. Après de brefs séjours à Saint-Louis et à Nouvelle-Orléans des États-Unis d'Amérique, il fut invité en 1955 à l'Observatoire de Géophysique du Collège Jean-de-Brébeuf qui en était à ses débuts. À ce dernier poste, comme directeur de la recherche, le Père Gherzi s'intéressa tout particulièrement au rayonnement solaire, à la propagation des ondes radio, à l'ionosphère et à l'électricité atmosphérique.

Au cours de sa longue carrière, il publia une centaine de volumes et brochures et autant d'articles dans diverses revues scientifiques.

Il était membre de l'Académie Pontificale des Sciences, de l'Académie des Sciences de Lisbonne et de l'Académie des Sciences de New York.

C.E., Montréal, P.Q.

The Use of Isentropic Coordinates in the Formulation of Objective Analysis and Numerical Prediction Models

M.A. Shapiro

*National Center for Atmospheric Research¹
Boulder, Colorado 80302*

[Manuscript received 28 January 1974]

1 Introduction

During the first two decades of numerical weather prediction (NWP) dynamical meteorologists have focussed their efforts upon the objective data analysis, simulation and numerical prediction of large scale (~ 4000 km) weather systems of middle and high latitudes. Though these techniques have shown steady improvement over the years, they have suffered from the deficiency of being unable to resolve the finer-scale atmospheric systems such as frontal cyclones, low-level and upper-level frontal zones and squall lines, which are the essential "weather producing" systems that operational meteorologists must deal with on a daily basis. The "weather forecaster" should be aware that these deficiencies in NWP were imposed by the core storage and speed limitations of the early electronic computer systems. Hence, the exclusion of small scale weather systems from early NWP was not the result of an unawareness on the part of the model builders but a constraint imposed by the technology of the times.

With the advent of increased computational speed and core storage of present day electronic computers, dynamical meteorologists are directing their efforts toward the development of fine-mesh limited-area numerical weather prediction models. The primary objective of this new direction in numerical modeling is to obtain increased accuracy in short-range (12 hr to 48 hr) weather forecasts by incorporating small-scale (frontal and meso-convective) dynamical and thermodynamical physics into the prediction models.

The current trend in fine-scale model development is one of increasing both the horizontal and vertical grid resolution of existing large-scale coarse-mesh models and applying the high-resolution fine-mesh model over limited regions of rich upper-air data coverage. These modeling efforts consist of solving the primitive equations of motion in coordinate systems with horizontal surfaces defined relative to a vertical coordinate of pressure, p , height, z , or sigma, σ , ($\sigma = P/p_0$ where p_0 is the pressure at the earth's surface).

An alternate approach to the problem of incorporating frontal-scale processes into numerical weather prediction models is currently being undertaken by the NCAR Small Scale Analysis and Prediction Project. The approach uses potential temperature, θ , as the vertical coordinate with respect to which both objective data analysis and numerical prediction models are being formulated.

The motivation for performing frontal-scale numerical weather prediction

¹The National Center for Atmospheric Research is sponsored by the National Science Foundation.

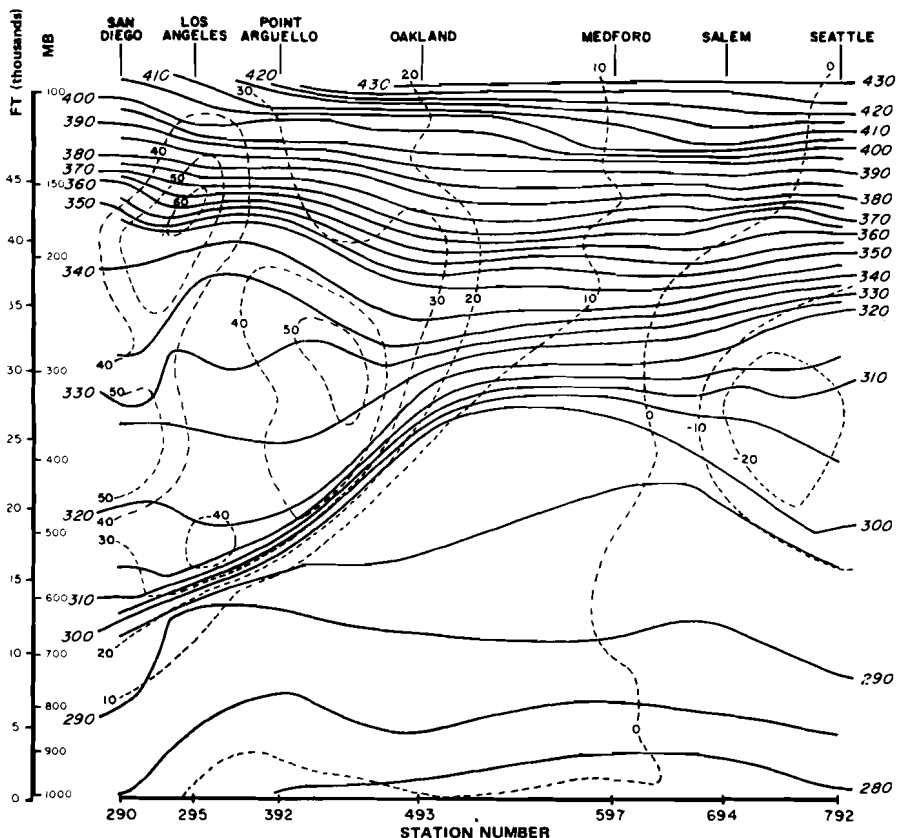


Fig. 1 Hand analyzed cross section of potential temperature, solid lines and observed wind speed, dashed lines through a middle-tropospheric frontal zone-jet stream system (after Duquet *et al.*, 1966).

on surfaces of constant potential temperature rather than on conventional z , p , or σ coordinate surfaces, stems from two basic properties of fronts. First, within frontal zones, the large-scale (~ 1000 km) variation of pressure and velocity on isentropic surfaces as compared to the small-scale (~ 100 km) variation of potential temperature and wind velocity on z , p , or σ surfaces (see Shapiro, 1970) permits the use of a coarse resolution horizontal mesh in θ -coordinates as compared to the required fine resolution mesh of conventional coordinate models. This may be seen in Fig. 1 by comparing the scale of the isentropic variation of pressure and wind velocity of the 310°K θ -surface situated within a strong middle-tropospheric frontal zone, with the scale of the variation of potential temperature and velocity on the 450-mb pressure surface which cuts across the 100-km wide frontal zone.

Secondly, a uniform vertical resolution (equally-incremented isentropic surfaces) θ -coordinate model is in effect a variable vertical resolution model in that frontogenesis and frontolysis appear as changes in separation distance between isentropic surfaces; i.e., in frontal regions with strong vertical gradients

the isentropic surfaces are closely packed, whereas in regions above and below fronts the isentropic surfaces become widely separated. This characteristic is illustrated in Fig. 1, where the vertical separation of 5°K increment isentropic surfaces ranges from 0.2 km within the frontal zone to 1 km on either side of the zone.

It is the purpose of this article to present a brief overview of some preliminary results of the isentropic coordinate approach to objective data analysis and numerical simulation of frontal zone-jet stream weather systems that is currently being undertaken at the National Center for Atmospheric Research.

2 Objective analysis in isentropic coordinates

Historically, synoptic meteorologists have used vertical cross-section analyses to specify the spatial and temporal distribution of temperature and wind velocity. The primary usefulness of this analysis tool lies in its ability to define frontal-scale horizontal gradients from the detailed vertical information content of synoptically-spaced upper-air observations. Fig. 1 shows an example of a hand-analyzed cross-section depicting frontal structure as taken from Duquet *et al.* (1966). The tedious and laborious nature of constructing such analyses has until now prevented their operational use by weather forecast centers.

In a recent study, Shapiro and Hastings (1973) developed an automated computerized routine for preparing objective cross-section analyses of potential temperature and geostrophic wind speed. The essence of the numerical technique is the use of Hermite polynomial interpolations to specify the distribution of pressure on isentropic surfaces between upper-air sounding reports. Vertical consistency between adjacent isentropic surfaces is imposed through Hermite interpolation of the inverse of thermal stability, $\partial p / \partial \theta$, on isentropic surfaces. The results of applying this computerized analysis scheme to the upper-air station data of Fig. 1 are presented in Fig. 2. A comparison between Figs. 1 and 2 reveals that the computerized isentropic scheme produces a frontal-scale potential temperature analysis which is nearly identical to the hand analysis. Furthermore, the objective scheme requires less than 1 second of CDC 6600 computer time, thus making possible its utilization in operational weather analysis and prediction.

The technique of imparting vertical consistency to isentropic coordinate objective analysis is being used to develop three-dimensional (x, y, θ) computerized analysis schemes which depict the three-dimensional temperature and velocity structure of middle-latitude weather systems containing fronts. The ability of these schemes to resolve frontal-scale gradients from synoptically-spaced observations is shown in Fig. 3, where the 500 mb potential temperature analysis was arrived at by coordinate transformation and interpolation from a coarse mesh (381 km grid resolution) multi-level (40 levels with 2½ °K resolution) isentropic analysis to a fine-mesh (64 km) constant pressure surface analysis. Prior to the development of these analysis techniques, it required months of hand analysis to depict the three-dimensional structure of fronts for a single synoptic map time. With the use of the computerized objective schemes, it is possible to perform the same task in 20 minutes of CDC 6600 computer time.

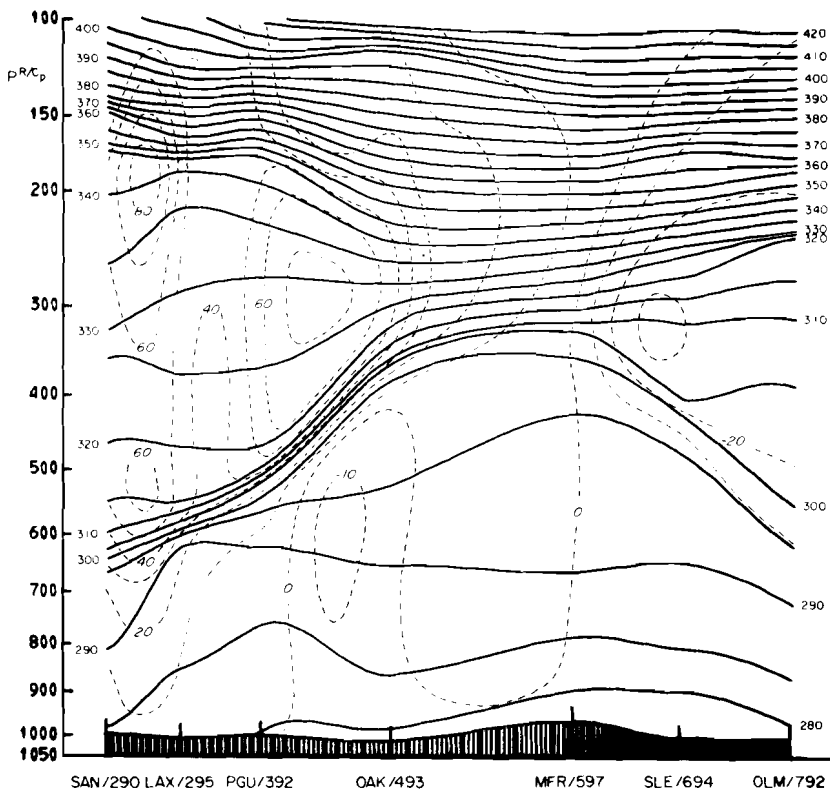


Fig. 2 Computer analyzed potential temperature and geostrophic wind velocity component for cross section data in Fig. 1.

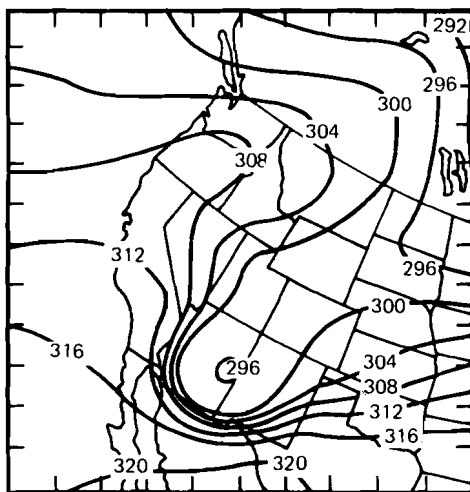


Fig. 3 Computer analyzed 500-mb potential temperature analysis ($^{\circ}\text{K}$) obtained from coordinate transformation (θ to p) of a 40-level three-dimensional isentropic coordinate objective analysis scheme.

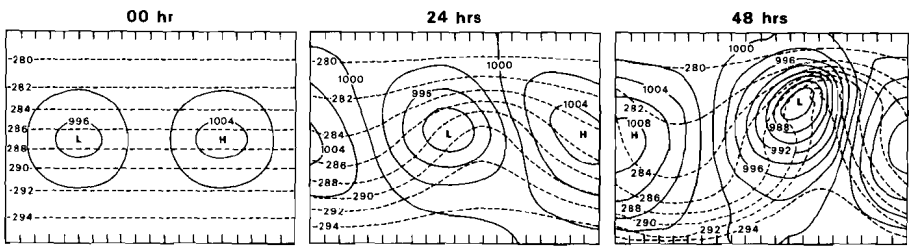


Fig. 4 Computer simulation of cyclogenesis and frontogenesis at the earth's surface. Isobars at 4 mb intervals, solid lines; isentropes at 2° K intervals, dashed lines.

3 Numerical weather prediction in isentropic coordinates

The isentropic coordinate approach to numerical weather prediction has received little attention during past years, because it was thought to contain several insurmountable problems. A primary difficulty, it was thought, would arise when isentropic surfaces intersect the earth's surface, resulting in numerical instabilities which would contaminate the forecast. This notion has since been dispelled by Eliassen and Raustein (1968, 1970), who have presented and tested a lower boundary condition on a six-level isentropic coordinate primitive equation model. Integrations out to 96 hours with one isentropic surface intersecting the ground gave rise to no instabilities at the intersection. It was also thought that the use of isentropic coordinates in a prediction model would result in an "entwining" of the integrating surfaces (generation of superadiabatic layers) which would destroy the forecast in a short number of time steps. This problem did not occur in either the six-level model of Eliassen and Raustein (1970) or the finer vertical resolution (20 levels) NCAR isentropic prediction model. Another possible difficulty usually cited is related to the methods of including diabatic processes and their effects in an isentropic coordinate model. Research by Deaven in the development of a diabatic boundary layer for isentropic coordinate models, and Bleck's efforts at inclusion of precipitation processes, are current NCAR efforts toward a solution of this problem.

Two approaches to performing numerical weather prediction in isentropic coordinates are currently under development by the NCAR Small Scale Analysis and Prediction group. The first, by Bleck (1973), uses filtered prediction equations which are initialized with the above described analysis scheme. The filtered model is based upon conservation of geostrophic potential vorticity and has been used to make daily 36-hr weather predictions on the NCAR 7600 and 6600 computers.

A second approach to isentropic numerical weather prediction by Shapiro and Kingry has been formulated using the primitive equations of motion. The prediction model is similar to that developed by Eliassen and Raustein (1970), with the addition that it contains 20 vertical levels, several of which intersect the ground topography. Results from a periodic lateral boundary condition (channel flow) version of this model have demonstrated its capability of generating fronts of a structure similar to those observed in the atmosphere. Fig. 4

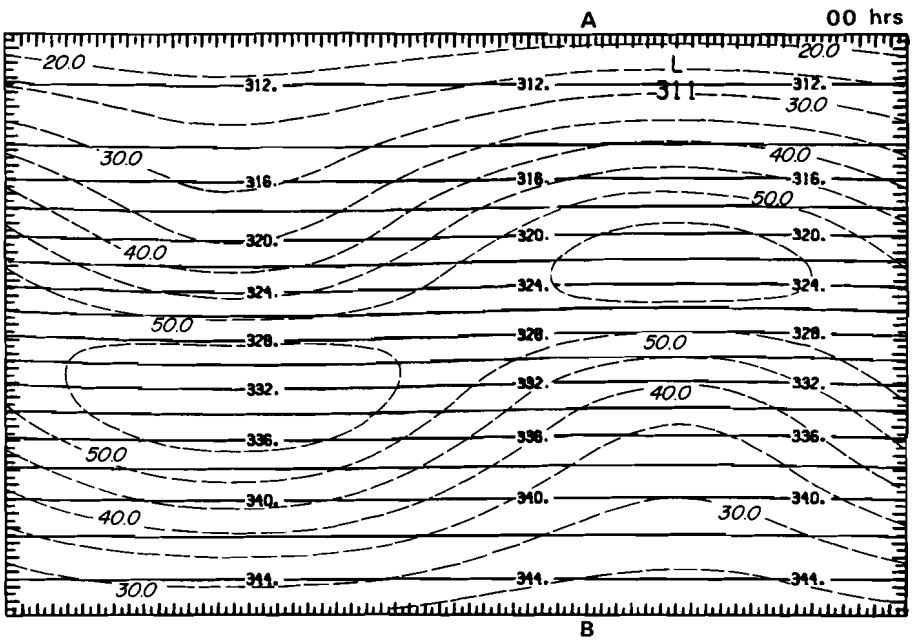


Fig. 5a

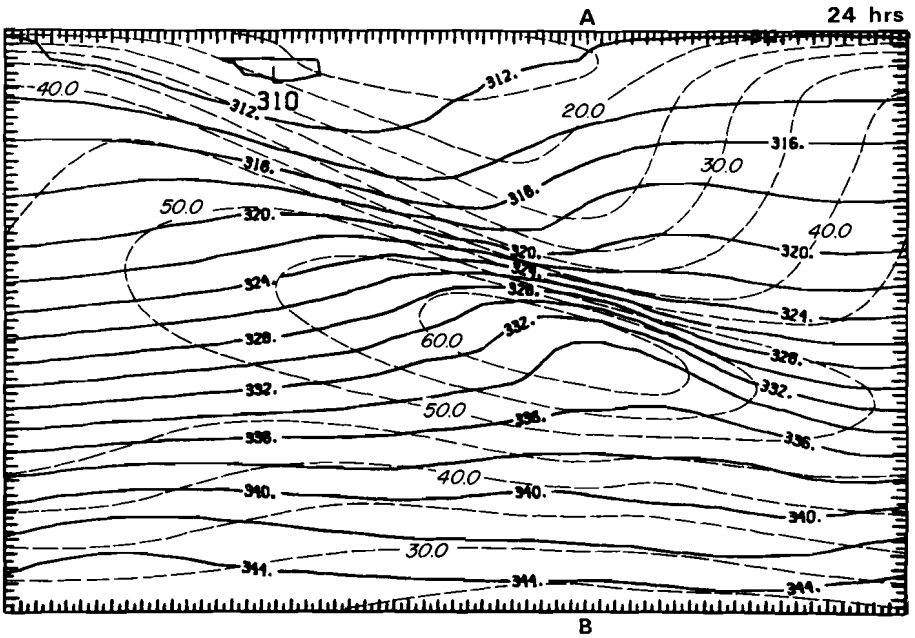


Fig. 5b

Fig. 5 Initial state 00-hr and 24-hr computer simulation of upper level frontogenesis at 350 mb as obtained by coordinate transformation (θ to p) from a 20-level isentropic coordinate primitive equation model. Potential temperature ($^{\circ}\text{K}$), solid lines; wind speed (m sec^{-1}), dashed lines.

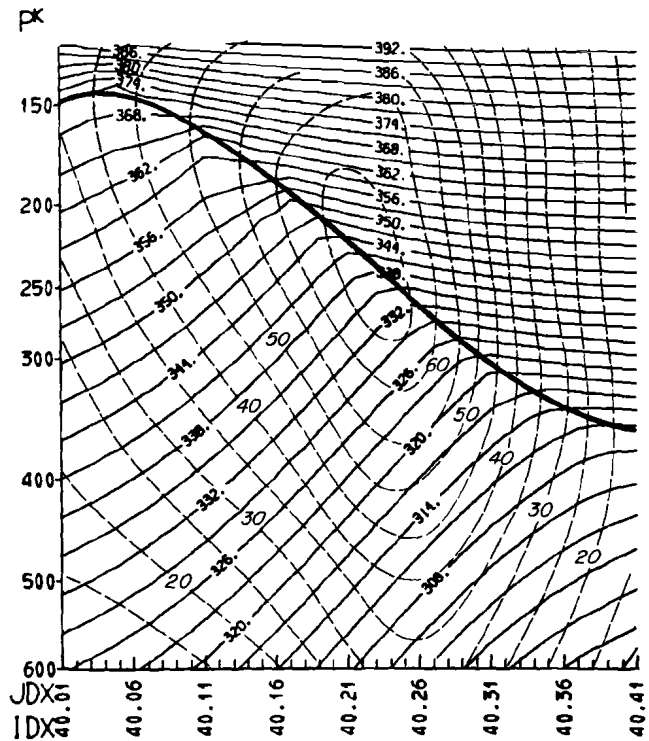


Fig. 6a

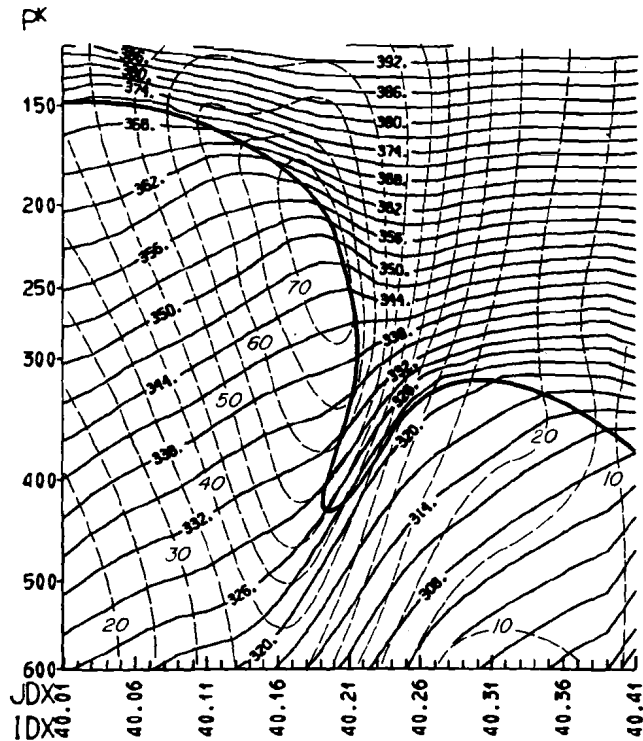


Fig. 6b

Fig. 6 Cross section of potential temperature, solid lines and wind speed at 00 and 24 hr as taken along the line between points A and B of Fig. 5, tropopause as defined by near zero order discontinuity of potential absolute vorticity, heavy solid line.

shows a simulation of low-level cyclogenesis and associated frontogenesis with this primitive equation model, where six isentropic surfaces intersect the ground with no resulting instabilities.

The ability of the isentropic-coordinate primitive-equation model to simulate upper-level frontogenesis is shown in Figs. 5 and 6. The frontogenesis in both the wind and potential temperature fields bears a striking similarity to that shown in the cross-section analysis of Fig. 1. Calculations of potential absolute vorticity demonstrate the model's realistic simulation of the stratospheric-tropospheric intrusion process with attendant frontogenesis as described by Reed and Danielsen (1959) and Danielsen (1964).

Starting in the winter of 1974, numerical weather forecasts will be made at NCAR using both filtered and primitive equation models in order to assess their utility for short range (12 to 48 hr) forecasts over the continental United States and southern Canada. Comparisons will be made with conventional models to determine if increased forecast accuracy of middle-latitude baroclinic weather systems is obtainable by framing both the objective analysis and prediction models in isentropic coordinates.

References

- BLECK, RAINER, 1973: Numerical forecasting experiments based on the conservation of potential vorticity on isentropic surfaces. *J. Appl. Meteor.*, **12**, 737-752.
- ELIASSEN, A., and E. RAUSTEIN, 1968: A numerical integration experiment with a model atmosphere based on isentropic coordinates. *Meteorologische Annalen*, **5**, 45-63.
- and ———, 1970: A numerical integration experiment with a six-level atmospheric model with isentropic information surface. *Meteorologische Annalen*, **5**, 429-449.
- DANIELSEN, E.F., 1964: Project Springfield report. Defense Atomic Support Agency, Report No. 1517, 97 pp.
- DUQUET, R.T., E.F. DANIELSEN, and N.R. PHAUS, 1966: Objectives cross section analysis. *J. Appl. Meteor.*, **5**, 233-245.
- REED, R.J., and E.F. DANIELSEN, 1959: Fronts in the vicinity of the tropopause. *Arch. Meteor. Geophys. Bioklim.*, **A11**, 1.
- SHAPIRO, M.A., 1970: On the applicability of the geostrophic approximation to upper-level frontal scale motions. *J. Atmos. Sci.*, **27**, 408-420.
- SHAPIRO, M.A., and J.T. HASTINGS, 1973: Objective cross-section analysis by Hermite polynomial interpolation on isentropic surfaces. *J. Appl. Meteor.*, **12**, 753-762.
-

An Operational Windchill Index

H. T. Beal

Prairie Weather Central, Winnipeg International Airport, Winnipeg, Canada

[Manuscript received 3 November, 1973]

ABSTRACT

The rate of heat loss from the human body by low temperatures and wind is commonly referred to as "Wind Chill". Traditionally the term means the rate of heat removal from the bare skin only. It neglects such important factors as clothing insulation, metabolic heat generation and sunshine. This paper presents a new windchill index

which includes the above parameters and discusses its advantages over the present concept of windchill. The principal advantage being that the new index may be directly correlated to human comfort or discomfort. In addition, the windchill may be adjusted for different clothing levels, metabolic rates, and solar radiation.

1 Introduction

Large areas in Canada experience severe winters. Temperatures of -30°C with windspeeds of 5 to 10 m/s are quite common over the prairies, for example. The rate of heat loss from persons under these environmental conditions is substantial. Under these conditions individuals who must go outdoors are attentive to the present temperature and windspeed and make a subjective estimate of the amount of clothing to wear. Naturally it would be desirable if weather offices could give the public a single index which would relate human comfort with the present or forecast temperature and windspeed. Preferably this index should indicate the amount of clothing to be worn and whether or not outdoor activity is feasible.

Thus personal comfort under a given set of environmental conditions (excluding psychological aspects) should be optimum when there is no net gain or loss of body heat.

In this report the author will endeavour to give a brief review of previous studies in this field and to suggest a more complete index for personal comfort than heretofore encountered in the literature.

2 Components of personal comfort

With the Canadian winter in mind, one can say that the thermal equilibrium of a person depends upon:

1. Metabolic heat production.
2. Radiative exchange with the environment and the sun.
3. Heat loss by convective processes.
4. Heat conduction to ground or other objects.
5. Heat loss through the lungs.

6. Effect of clothing to reduce convective, radiative, and conductive heat losses.
7. Physiological variables such as sex, age, health, time of food ingestion, and time of day.
8. Psychological effects such as length of darkness, snow and general state of mind.

3 History

As human discomfort during winter conditions is a difficult parameter to express mathematically, formulas have been developed to relate personal discomfort to the rate of heat loss Q from the body.

Now many of the early experiments produced relationships of the form

$$Q = h(T_s - T),$$

where Q is the rate of heat loss (windchill) in kcal/m² hr, T_s and T the skin surface and ambient air temperature, respectively in °C. The heat transfer coefficient is

$$h = a + bV^n + cV^m,$$

where a , b and c are constants, V the windspeed (m/s) and n and m are exponents. The various forms of h are illustrated in Table 1. These relationships were obtained by recording the cooling rate of various spheres and cylinders (diameters in the range 2 to 8 cm) under different temperatures and windspeeds.

Of all expressions the one devised by Siple is still in widespread use to determine the feasibility of outdoor activity (especially in military operations). A basic fault of Siple's windchill is that it underestimates the windchill at high wind speeds. Substitution shows that the heat loss reaches a maximum at 25 m/s

TABLE 1. Comparison of experimental formulas for $Q = (a + bV^n + cV^m)(T_s - T)$.

Researcher	a	b	n	c	m	T_s °C
1 Hill	4.68	16.92	0.50	—	—	36.5
2 Weiss	5.04	17.64	0.50	—	—	36.5
3 Lehmann	4.07	12.24	0.7-0.8	—	—	36.5
4 Dorno	7.92	9.00	0.667	—	—	33.0
5 Huttner	8.28	16.92	0.52	—	—	36.5
6 Siple and Passel						
1945	10.45	10.00	0.50	-1.00	1	33.0
7 Plummer						
1944	0.31	8.32	0.50	+1.86	1	33.0
8 Winslow <i>et al.</i>						
1939	3.40	10.60	0.50	—	—	33.0

For researchers 1 to 5 see Court (1948). Here Q is in units of kcal/m² hr and V , in m/s, the wind speed. T_s and T are the skin and ambient air temperatures, respectively in °C.

(56 mph) so that some windchill tables claim little additional cooling at winds in excess of 40 mph.

One should note that the equations in Table 1 only give the heat loss due to convection from the bare skin. Consequently these relations can only give an estimation of heat losses from the face and hands which are usually exposed. The traditional windchill then tends to exaggerate the actual heat loss from an adequately dressed person. Persons dressed for an arctic environment may survive extreme conditions for several days.

A more operationally oriented definition of windchill would have to be based upon an equation of energy exchange, viz.,

$$Q = A - B,$$

where A represents the total rate of heat loss and B the total rate of heat input with Q being the net rate of heat gain or loss (new windchill). Ideally the terms A and B should include all factors of personal comfort listed before. Naturally this index would be somewhat more subjective than the traditional Siple windchill. However it would be more advantageous in defining the current weather conditions relative to a suitably dressed man. This approach is not new. Auliciems *et al.* (1973) and Steadman (1971) both developed an equation of energy exchange which included the effects of clothing insulation. They thought that the clothing thickness required to maintain the body in thermal equilibrium (i.e., $A = B$) would be a useful index. On a day to day operational basis clothing thicknesses would often reach an extreme value (under rare occasions a zero or negative value would occur). This information if passed directly to the public may be of dubious value. Better would be a figure giving the net loss or gain of heat from an adequately dressed man. This type of index would immediately convey that for $Q > 0$ an average person would become increasingly colder. While for $Q < 0$ he would be warm and at $Q = 0$ just comfortable. Furthermore the equivalent windchill temperature may accompany this index. For a given set of conditions (i.e., temperature, wind speed, clothing thickness etc.) there is a certain rate of heat exchange with the environment. Equivalent temperature is then that temperature which the air must have in order to produce this same rate of heat exchange but with very light wind speeds. These equivalent temperatures computed from Siple's formula are quite often broadcast to the public. For example at 0°F with a wind speed of 10 and 20 mph the equivalent windchill temperature is -15 and -32°F respectively. Again it is doubtful whether these are the effective temperatures experienced by a suitably clothed man.

4 The model

To provide a consistent framework we will omit any psychological effects as they are extremely variable. Physiological variables such as sex and state of health will be combined under the assumption we are dealing with an "average" person. Furthermore, we assume that the person is wearing appropriate winter clothing.

a *Clothing distribution*

Let the face be uncovered and represent 3% of body surface. Hands occupy 5% of the body surface and are covered with clothing of less thickness than the bulk of the body. The feet represent 7% of the body surface and also are covered with material less thick than the bulk of the body. The remaining 85% is well covered with appropriate clothing.

b *Clothing insulation*

The insulation of clothing depends on many factors, for instance thickness, texture and number of layers. In addition other parameters such as sweating, air spaces between layers and the bellows effect when a person moves (Belding *et al.*, 1947) also affect the insulating properties of clothing. For the sake of simplicity we will neglect these additional complications. The model will have two separate clothing assemblies. One will consist of heavy underwear, shirt and trousers, woollen coveralls and a hooded parka for severe cold weather. We will assume an overall thickness of 2.5×10^{-2} m having an effective resistance of $0.72 \text{ m}^2 \text{ hr } ^\circ\text{C}/\text{kcal}$ (thermal conductivity $0.0347 \text{ kcal m}/\text{m}^2 \text{ hr } ^\circ\text{C}$).

A clothing assembly appropriate to more moderate conditions will consist of cotton underwear, a shirt, a suit and a heavy overcoat. An overall thickness of 1.0×10^{-2} m with an average resistance of $0.252 \text{ m}^2 \text{ hr } ^\circ\text{C}/\text{kcal}$ (thermal conductivity $0.040 \text{ kcal m}/\text{m}^2 \text{ hr } ^\circ\text{C}$) is assumed (see Morris, 1955; and Fourt and Harris, 1949).

In both cases the model is assumed to wear a good pair of mittens with resistance $0.18 \text{ m}^2 \text{ hr } ^\circ\text{C}/\text{kcal}$. The feet are covered with woollen socks and leather boots having a total resistance of $0.14 \text{ m}^2 \text{ hr } ^\circ\text{C}/\text{kcal}$.

c *Body and skin temperatures*

Body temperatures are generally about 37°C . The skin temperature of the torso is usually lower. Gage *et al.* (1941) and Belding *et al.* (1947) both indicate that under normal activity and with adequate clothing the skin temperature is approximately 33°C . Following Steadman (1971) the temperature of the face, hands, and feet is taken as 30°C . These members are generally a few degrees cooler than the skin with no discomfort.

d *Metabolic heat production*

When outdoors, a person expends a certain amount of energy which helps to maintain thermal equilibrium. For example, a man sitting or standing expends approximately 50 to $70 \text{ kcal}/\text{m}^2 \text{ hr}$. Furthermore, walking (2 mph) and shovelling correspond to a rate of heat generation of 100 and $450 \text{ kcal}/\text{m}^2 \text{ hr}$, respectively (from Newburgh, 1949 and Fourt and Hollies, 1969). Clearly it would be cumbersome to compute the windchill for many different rates of energy production. However it would be useful to compute windchill for three main activities common to the general public. A rate of $60 \text{ kcal}/\text{m}^2 \text{ hr}$ is chosen for such activities as waiting for a bus or watching an outdoor game. A second category consists of light activity (i.e., walking to one's car, brushing

snow off wind-shield) with an energy expenditure of 120 kcal/m² hr. Lastly, a rate of 300 kcal/m² hr is chosen to represent the expenditure due to outdoor construction work, shovelling snow and so forth.

e Heat loss from lungs

Assuming an overall breathing rate of 0.79 kg of air per hour per sq. m of body surface and that the air is exhaled at body temperature (37°C) gives a rate of heat loss

$$Q = h_1(37 - T),$$

where $h_1 = 0.188 \text{ kcal/m}^2 \text{ hr } ^\circ\text{C}$.

In addition there is evaporative heat loss from the lungs. Winter air is quite dry, say, 0.004 kg of water vapour per kg of dry air. After its passage through the lungs the moisture content is somewhat less than saturated air at body temperature. Roughly the increase of specific humidity may be taken as 0.030. The evaporative heat loss, with latent heat of evaporation 570 kcal/kg, thus becomes

$$Q_e = 570(0.79)(0.30) = 13.50 \text{ kcal/m}^2 \text{ hr}.$$

f Solar radiation

Besides the metabolic heat production a person will receive a small amount of solar radiation. This quantity of short wave radiation absorbed by the body is quite variable and small in relation to the internal heat generation. However on a calm sunny day this amount of solar radiation is significant. Many variables such as solar declination, atmospheric turbidity, cloud cover, latitude, reflectivity of environment, exposed surface area of man, reflectivity and absorptivity of clothing worn will affect the additional solar heat input. More precise methods of computing this heat input exist (Roller and Goldman, 1968) than the one formulated below. However, in an operational environment only those variables readily accessible may be used.

As a first approximation, the rate of heat input from solar radiation is

$$Q_s = p^m I_o,$$

where I_o is the solar constant (1200 kcal/m² hr) and p the mean zenith path transmissivity of the atmosphere with m the optical air mass. For latitudes 50 to 60° during the fall, winter and spring months an average value of 0.72 may be substituted for p^m (Auliciems *et al.*, 1973).

Of the amount of direct sunlight only 50% falls on the total body surface (Underwood and Ward, 1960; Roller and Goldman, 1968). In the above figure about 15% has been added to account for reflected and diffuse radiation. Of this amount we assume that 80% is absorbed by the clothing worn and the bare skin.

Hay (1970) (see Auliciems *et al.*, 1973) estimated that the amount of direct sunlight is reduced by cloud cover by the factor $(1 - C^{1.33})$ where C is the cloud cover in tenths.

Furthermore, the equation for solar radiation must also be multiplied by the factor

$$\cos(\phi - \delta)$$

in order to obtain the radiation flux normal to the earth's surface at latitude ϕ with the sun's declination δ . The measurements are made at noon in order to neglect the hour angle. Assuming an average latitude of 55° and a declination of -10° for the winter months the factor simply becomes $\cos(65) = 0.42$ (Garnier and Ohmura, 1968).

Taking into consideration all the above factors, the net rate of heat input from the sun becomes

$$\begin{aligned} Q_s &= 0.42 (0.8) (0.5) (0.72) (1200) (1 - C^{1.33}), \\ &= 144 (1 - C^{1.33}), \text{ kcal/m}^2 \text{ hr.} \end{aligned}$$

g Radiative heat loss

The human body continuously radiates heat at long wavelengths. Especially during calm, very cold days this mechanism may well contribute significantly to the windchill.

Ordinary clothing and human skin have an emissivity of approximately unity. Thus the rate of heat loss is given by the Stefan Boltzmann Law, viz.

$$Q_r = \sigma(T_s^4 - T^4),$$

where σ is the Stefan Boltzmann constant ($4.88 \times 10^{-8} \text{ kcal/m}^2 \text{ hr } ^\circ\text{K}^4$), and T_s and T the body surface and ambient air temperature ($^\circ\text{K}$) respectively. The above equation may be rewritten more conveniently as,

$$Q_r = h_r(T_s - T),$$

with

$$h_r = 4.88 \times 10^{-2} \left[\left(\frac{T_s + 273}{100} \right)^2 + \left(\frac{T + 273}{100} \right)^2 \right] \left[\frac{T_s + 273}{100} + \frac{T + 273}{100} \right],$$

and where h_r is the radiative heat transfer coefficient ($\text{kcal/m}^2 \text{ hr } ^\circ\text{C}$) and with the temperatures in $^\circ\text{C}$.

h Conductive heat loss

Another avenue of heat loss is through the soles of boots by conduction. Here the rate of heat loss is simply

$$Q_b = h_b(T_s - T),$$

where h_b is the heat transfer coefficient of the soles (i.e. the reciprocal of the thermal resistance). T_s is the surface temperature of the soles while T is the ground temperature which may be approximated by the ambient air temperature.

i Convective heat loss

Convection involves the heat transfer by the mixing of one parcel of air by

the other. The convective transfer of heat is the most important process in cooling the human body as well as the most complex. For a stationary person and with light winds (0 to 2 m/s) the convective mechanism is mainly the result of differences of density resulting from the temperature gradient between the body and the air (natural convection). On the other hand, stronger winds markedly increase the heat transfer rate (wind-forced convection). Effectively the thermal conductivity of the air increases due to increasing turbulence about the body.

Natural convection

Many investigations have been done with heated plates and cylinders on this phenomenon (McAdams, 1954). Furthermore, these studies indicate that the heat transferred by natural convection is comparable to that by radiation. Treating the clothed person, to a first approximation, as a small upright cylinder, the rate of heat loss is given by

$$Q_n = h_n(T_s - T),$$

where

$$h_n = 2.09(T_s - T)^{1/4}.$$

Again T_s and T are the surface and ambient air temperature ($^{\circ}\text{C}$) respectively. The heat transfer coefficient h_n of natural convection ($\text{kcal/m}^2 \text{ hr } ^{\circ}\text{C}$) is a very complex function of the cylinder diameter, Nusselt, Grashof and Prandtl numbers. The particular value chosen for h_n assumed a turbulent boundary layer for the air flowing upwards along the body (McAdams, 1954).

Forced convection

The heat transfer coefficient for forced convection is very dependent upon the wind speed. It is well known that the wind speed varies considerably with height (Johnson, 1959), as well as terrain. Meteorological observations of wind speed are made over a wide range of elevations (for example, at the Winnipeg Airport the wind speed is recorded at 20 m above ground). The variation of wind speed, near the ground, with height is generally given by a power law of the form,

$$V_1 = V_0(Z_1/Z_0)^n,$$

where V_1 is the wind speed a distance Z_1 above ground with V_0 the recorded wind at a height Z_0 . Buckler (1969) investigated this variation of wind speed with height over the Prairies and found exponents in the range of 0.15 to 0.30.

Taking an average exponent of 0.25, a mean anemometer height (Z_0) of 10 m, and 1.7 m as the average height of an adult, the average wind speed felt will be

$$V = (V_0/1.7) \int_0^{1.7} (Z/10)^{0.25} dz,$$

$$V = 0.51 V_0.$$

Clearly, neglect of this fact would overestimate the actual amount of windchill.

The heat loss due to forced convection is simply,

$$Q_c = h_c (T_s - T).$$

All investigators agree that the rate of heat loss is proportional to the temperature difference but no exact expression exists for h_c . Instead of choosing an expression for h_c from Table 1, we prefer a relationship of the form

$$N_u = C R_e^m$$

where N_u is the Nusselt number and R_e the Reynolds number with C and m constants. A large number of investigators, notably Hilpert (See Eckert, 1959) have studied the heat transfer by forced convection from heated cylinders. Thus approximating the human body by an upright long cylinder of say 10 cm diameter the results of these studies may be applied. For wind speeds of the order of 10 m/s and the above cylinder diameter, the Reynolds number is of the order 10^4 . Hilpert's results ($R_e \sim 10^4$) for a circular cylinder are $C = 0.0239$ and $m = 0.805$; and for an octagonal cylinder $C = 0.0347$ and $m = 0.782$. These results are also corroborated by Steadman (1971).

Following Steadman the relation

$$N_u = 0.04 R_e^{0.75}$$

was used. Substitution of the necessary values for air at 0°C yields

$$h_c = 6.27 V^{0.75},$$

where h_c is in units of $\text{kcal/m}^2 \text{ hr } ^\circ\text{C}$ and the wind speed in m/s. Now V is the wind speed experienced by the body and changing this to the wind speed reported at anemometer height yields

$$h_c = 3.79 V_o^{0.75}$$

5 The windchill equation

Defining, for ease of manipulation,

$$R = 1/(h_r + h_c + h_n P),$$

the total resistance due to radiation and convection. The parameter P is zero for $V_o > 2$ m/s and unity for $V_o \leq 2$ m/s. In terms of the wind speed and temperature the above expression becomes

$$R^{-1}(V_o, T_s, T) = 4.88 \times 10^{-2} \left[\left(\frac{T_s + 273}{100} \right)^2 + \left(\frac{T + 273}{100} \right)^2 \right] \\ \cdot \left[\frac{T_s + 273}{100} + \frac{T + 273}{100} \right] + 3.79 V_o^{0.75} + 2.09 P (T_s - T)^{\frac{1}{2}}$$

$\text{kcal/m}^2 \text{ hr } ^\circ\text{C}$. The temperatures T_s and T are in $^\circ\text{C}$ with V_o in m/s.

The rate of heat loss from the lungs (due to warming of outside air and evaporation) is

$$13.50 + 0.188(37 - T) \text{ kcal/m}^2 \text{ hr},$$

from the face

$$(30 - T)/R(V_o, 30, T) \text{ kcal/m}^2 \text{ hr,}$$

from the hands

$$(30 - T)/[R(V_o, T + 5, T) + 0.18] \text{ kcal/m}^2 \text{ hr,}$$

from the feet

$$(30 - T)/0.14 \text{ kcal/m}^2 \text{ hr,}$$

from the torso

$$(33 - T)/[R(V_o, T + 5, T) + R_o] \text{ kcal/m}^2 \text{ hr.}$$

Here R_o is the resistance of the clothing covering the torso, being $0.72 \text{ kcal}^{-1}\text{m}^2 \text{ hr } ^\circ\text{C}$. Furthermore, the temperature difference between the outer surface of the clothing and the ambient air is usually about 5°C (Belding *et al.*, 1947). Thus we assume that the surface temperature of the clothing is $(T + 5)^\circ\text{C}$.

The total rate of heat energy input is

$$Q_i = M + 144(1 - C^{1.33})\bar{R} \text{ kcal/m}^2 \text{ hr,}$$

where M is the metabolic rate taken as 60, 120 and 200 $\text{kcal/m}^2 \text{ hr}$ for light moderate and strenuous activities, respectively. The second term representing the solar input with C the cloud cover in tenths. The factor \bar{R} is the overall resistance,

$$\bar{R} = 0.03 + \frac{0.05R(V_o, T + 5, T)}{R(V_o, T + 5, T) + 0.18} + \frac{0.92R(V_o, T + 5, T)}{R(V_o, T + 5, T) + R_o}.$$

The amount of solar energy absorbed, Q_s , by the face, hands and torso must be reduced by the above terms, for the amount of solar heat input that actually reaches the skin will depend upon the clothing insulation as well as the heat dissipation at the outer clothing surface.

Combining the above terms, the new windchill factor becomes

$$Q = 13.50 + 0.188(37 - T) + [0.03/R(V_o, 30, T) + 0.05/(R(V_o, T + 5, T) + 0.18) + 0.07/0.14](30 - T) + 0.85(33 - T)/(R(V_o, T + 5, T) + R_o) - Q_i.$$

6 Results and discussion

From the development of the windchill equation it appears that this model will provide a single realistic measure of climatic severity. However, one must note that the large number of variables involved in determining personal comfort limit the applicability of the results obtained. This windchill index is considerably more flexible than one based upon temperature and wind speed alone. For example, suppose that the windchill is to be computed at various localities across the Prairies. First, the formula allows one to account for the different heights at which the wind speed is recorded as well as to vary the

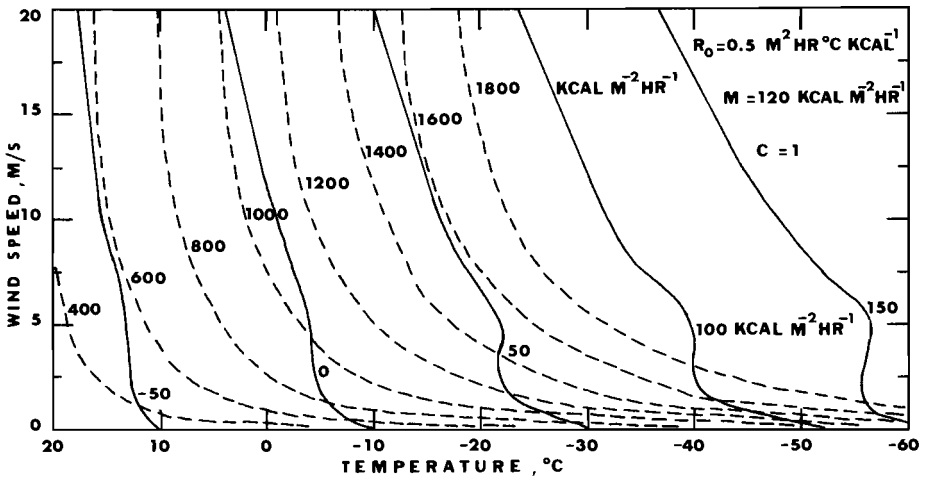


Fig. 1 A comparison of the Siple windchill isopleths (dashed lines computed from Siple's formula in Table 1) with the new windchill isopleths (solid lines) for a given metabolic rate (M), clothing resistance (R_0) and an overcast sky.

exponent in the wind power law according to the terrain roughness. Furthermore, the average clothing thickness and the mean metabolic rate may be adjusted for the different regions to reflect the severity of the climate and the main occupation of the community. In other words the windchill index may be tailored to specific regions as well as certain occupations.

Fig. 1 illustrates the windchill isopleths as a function of temperature and wind speed. It is assumed that the model is engaged in moderate activity and wears an arctic uniform (i.e., heavy underwear, good parka with hood, gloves and lined boots). The zero windchill isopleth implies no net heat loss so that for any combination of temperature and wind speed yielding this isopleth the model should be wholly comfortable. The Siple windchill isopleths (dashed lines) are also illustrated. We immediately note that at very light windspeeds these isopleths are somewhat suspect. Windchill nearly doubles when the wind speed increases from say 1 to 2½ m/s. In addition, at very high wind speeds the cooling rate remains almost constant with further increasing winds.

The behaviour of the 0 and 100 kcal/m² hr windchill isopleths for various metabolic rates and clothing resistances is shown in Fig. 2. This graph simply indicates that to maintain the given amount of windchill under different environmental conditions either the metabolic rate or clothing thickness or both must be altered.

Currie (1951) made a study of the different levels of comfort experienced by indoor workers when briefly exposed to various temperatures and wind speeds (the subjects were dressed in normal winter clothing). Three of his sensation isopleths are shown in Fig. 3 together with the windchill isopleths. Clearly there is a good correlation between windchill and sensation for wind-speeds up to about 8 m/s after which Currie's results were uncertain. However,

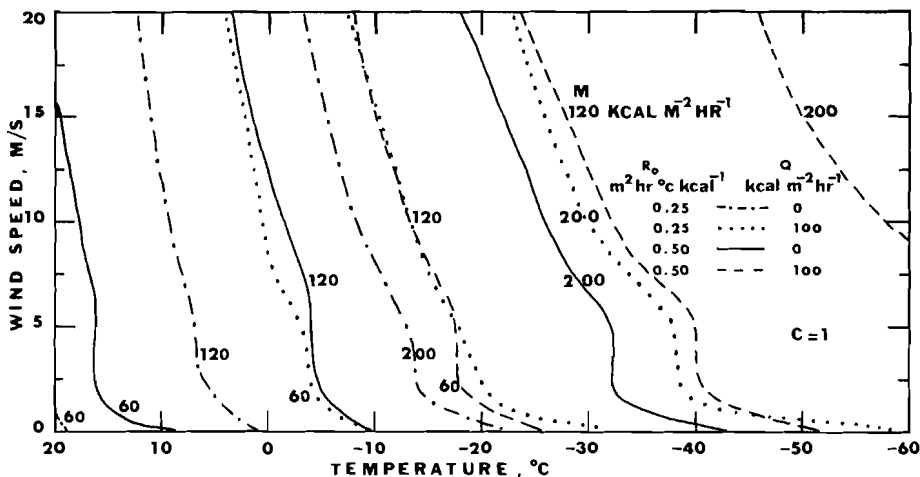


Fig. 2 The behaviour of the windchill (Q) isopleths as a function of windspeed and temperature, for different metabolic rates (M) and clothing resistances (R_0) under an overcast sky.

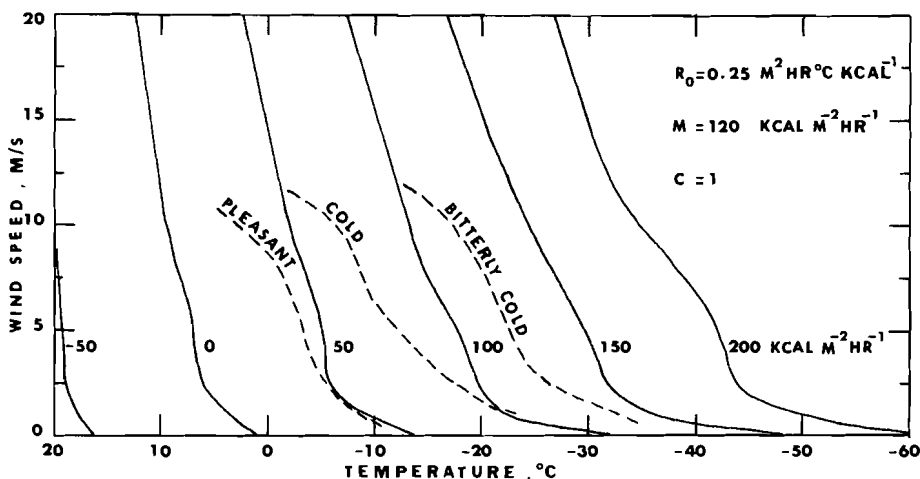


Fig. 3 Windchill isopleths as a function of windspeed and temperature. The dashed lines are sensation isopleths after Currie (1951).

the results do show that the windchill values lie within the correct range. The different ranges of comfort corresponding to windchill are indicated on Fig. 4. The model would feel warm to cool for a windchill of -50 to $+50$ kcal/m² hr, respectively. The lines of constant wind speed (dashed) as a function of temperature and windchill are for moderate activity and ordinary winter clothing. It should be noted that taking a wind speed and temperature and observing the sensation from Fig. 3, that the sensation falls into the proper category on Fig. 4. As a further test of the applicability of the formula, solid lines of

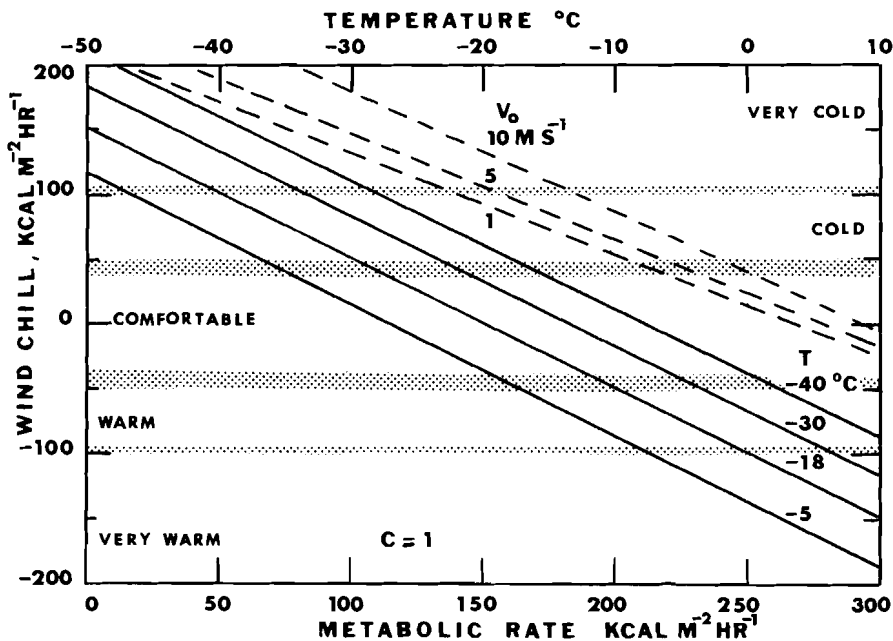


Fig. 4 The solid lines are temperature isopleths as a function of windchill and metabolic rate for a clothing resistance of $0.50 \text{ m}^2 \text{ hr } ^\circ\text{C/kcal}$ and a windspeed of 1 m/s . The dashed lines give the behaviour of the windchill and temperature for various windspeeds (V_0) with a clothing resistance of $0.25 \text{ m}^2 \text{ hr } ^\circ\text{C/kcal}$ and a fixed metabolic rate of $120 \text{ kcal/m}^2 \text{ hr}$. The graph illustrates the correlation between windchill and personal comfort; see text for discussion.

constant temperature were drawn on Fig. 4 as a function of windchill and metabolic rate. The model was assumed to wear an arctic uniform and experience a light wind. Belding *et al.* (1947) performed tests on men heavily clothed performing various activities at low temperatures. The results indicated that at -18°C with metabolic rates 50, 120, 200 and $300 \text{ kcal/m}^2 \text{ hr}$ the subject felt cold, cool, comfortable and hot, respectively. These sensations when translated into windchill by Fig. 4 fall indeed into the proper ranges.

It should be apparent that under severe conditions no amount of clothing by itself is sufficient to keep the model warm. This effect is observed by football spectators, and snowmobilers and others whose metabolic output is low.

In summary, a windchill index of this kind may provide a useful index as to the severity of the environment under a wide range of conditions. From an operational viewpoint, the windchill is easily computed from hourly observations and may be given in short-term forecasts. Furthermore, it is adaptable to specific requirements.

Acknowledgments

The author is pleased to have been supported in this study by the Prairie Weather Central and its computing facilities.

References

- AULICIEMS, A., C.D. DE FREITAS and F.K. HARE, 1973: Winter Clothing requirements for Canada. *Climatological Studies*, **22**, 80 pp., Environment Canada.
- AULICIEMS, A., and F.K. HARE, 1973: Weather forecasting for personal comfort. *Weather*, **28**, 118-121.
- BELDING, H.S., H.D. RUSSELL, R.C. DARLING and G.E. FOLK, 1947: Thermal responses and efficiency of sweating when men are dressed in arctic clothing and exposed to extreme cold. *Amer. J. Physiol.*, **149**, 233-239.
- BUCKLER, S.J., 1969: The vertical wind profile of monthly mean winds over the Prairies. *Canada Department of Transport. Tech. Memo.*, TEC 718, 16 pp.
- COURT, A., 1948: Wind Chill. *Bull. Amer. Meteorol. Soc.*, **29**, 487-493.
- CURRIE, B.W., 1951: Sensation isopleths on a wind-temperature diagram for winter weather on the Canadian Prairies. *Bull. Amer. Meteorol. Soc.*, **32**, 371-374.
- ECKERT, E.R.G., 1959: *Heat and Mass Transfer*, McGraw-Hill, p. 242.
- FOURT, L., and M. HARRIS, 1949: *Physiology of Heat Regulation and the Science of Clothing*. Newburgh, L.H., ed., W. B. Saunders, Philadelphia, 291-319.
- FOURT, L., and N. HOLLIES, 1969: The comfort and function of clothing. U.S. Army Natick Laboratories, Mass., TEC 6974-CE.
- GAGGE, A.P., A.C. BURTON and H.C. BAZETT, 1941: A practical system of units for the description of the heat exchange of man with his environment. *Science*, **94**, 428-430.
- GARNIER, B.J., and A. OHMURA, 1968: A method of calculating the direct short wave radiation income of slopes. *J. Appl. Meteorol.*, **7**, 796-800.
- JOHNSON, O., 1959: An examination of the vertical wind profile near the ground. *J. Appl. Meteorol.*, **16**, 144-148.
- MCADAMS, W.H., 1954: *Heat Transmission*, 3rd ed., McGraw-Hill, 532 pp.
- MORRIS, M.A., 1955: Thermal insulation of single and multiple layers of fabrics. *Textile Research J.*, **25**, 733-766.
- NEWBURGH, L.H., 1949: *Physiology of Heat Regulation and the Science of Clothing*. Saunders, Philadelphia, p. 448.
- ROLLER, W.L., and R.F. GOLDMAN, 1968: Prediction of solar heat load on man. *J. Appl. Physiol.*, **24**, 717-721.
- SIPLE, P.A., and C.F. PASSEL, 1945: Measurements of dry atmospheric cooling in sub-freezing temperatures. *Proc. Amer. Phil. Soc.*, **89**, 177-199.
- STEADMAN, R.G., 1971: Indices of windchill of clothed persons. *J. Appl. Meteorol.*, **10**, 674-683.
- UNDERWOOD, C.R., and E.J. WARD, 1960: The radiation area of the erect human body with respect to the sun. *Proc. Third Intern. Congress on Photobiology*, p. 353.

The Correlation of Snowpack with Topography and Snowmelt Runoff on Marmot Creek Basin, Alberta

Douglas L. Golding

Northern Forest Research Centre, Edmonton, Alberta

[Manuscript received 17 March 1973; in revised form 4 February 1974]

ABSTRACT

In a model relating snow water equivalent to 6 combinations of topographic and forest variables on Marmot Creek experimental basin, 36 per cent of the variance was accounted for. The model was improved by the addition of a variable indexing position of snow-sampling points relative to major topographic features of the basin. Variation accounted for in the final model was 48 per cent.

To determine how well snow courses that have been measured for the past ten years indexed actual snow accumulation, snow-course data were correlated with mean snow water

equivalent measured in 1969-72 at 1500 points spaced on a 20.1 m × 201.2 m grid over the basin. Correlation coefficients ranged from 0.95 to 0.99 with particular courses consistently being the highest, indicating that these courses do provide a good index of basin snowpack.

Seasonal streamflow from Marmot and its three sub-basins was correlated with snow accumulation. Correlation was higher for the relation of snow accumulation with May-June runoff than with May-July runoff. Correlation coefficients ranged from 0.73 to 0.94 for the seven snow courses.

1 Introduction

Marmot Creek experimental watershed is a 9.4 km² basin on the west side of the Kananaskis River Valley, about 40 km southeast of Banff, Alberta. The basin consists of three sub-basins and an area below their confluence (Fig. 1). Topography is steep and elevation ranges from 1,585 to 2,805 m a.s.l. Forest cover is mainly Engelmann spruce (*Picea engelmanni* Parry), alpine fir (*Abies lasiocarpa* (Hook.) Nutt.) and lodgepole pine (*Pinus contorta* Dougl. var *latifolia* Engelm.) with timberline about 2,300 m.

Marmot Creek was established as an experimental watershed in 1961, one of the main objectives being to determine the effect of commercial timber harvest on basin hydrology. The intention was to develop methods for managing the forest for water as well as the other products of the forest. One direct hydrologic effect of manipulating forest cover on the east slopes of the Rocky Mountains is on snow accumulation and snowmelt rates.

The objectives of the present study are (1) to determine what topographic and forest variables affect snow accumulation, (2) to determine how well the

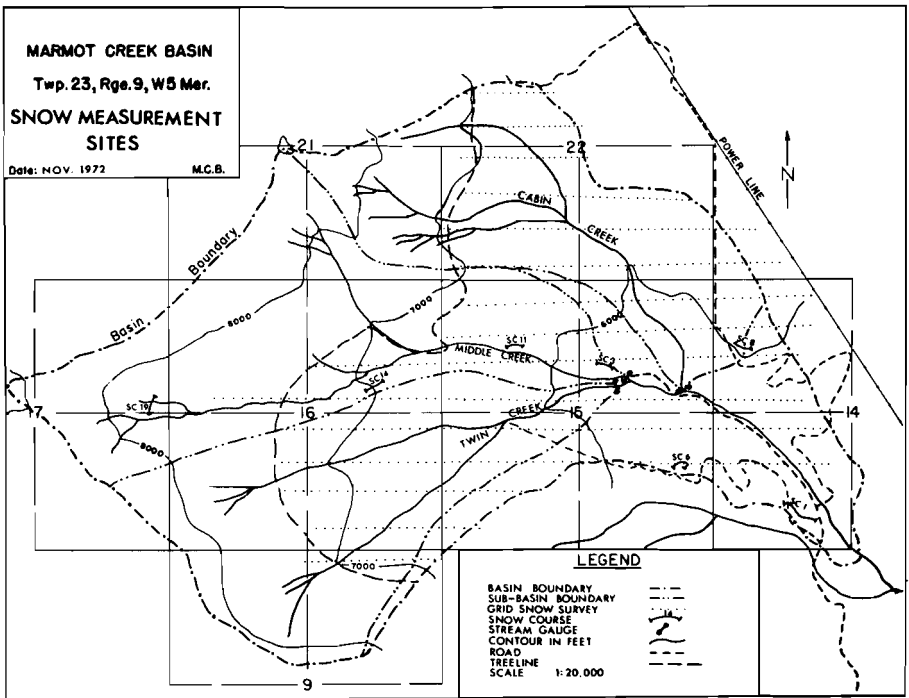


Fig. 1 Snow courses and grid sampling locations on Marmot Creek experimental watershed.

snow courses index snow accumulation on the basin, and (3) to relate runoff from the basin during snowmelt to snow accumulation.

2 Review

Snow Accumulation Model

Snow accumulation has been related to topographic and forest variables in other studies. The variables that exhibit the strongest relationship to snow accumulation vary from one situation to another. Packer (1962) constructed a model in which the independent variables of elevation, aspect, and forest cover accounted for over 90% of the variance in snow accumulation. A model constructed by Anderson (1967) explained 82% of the variance using only storm characteristics such as precipitation at index station and wind. Ffolliott and Hansen (1968) related snow accumulation to forest density, elevation, and potential insolation. Forty-six per cent of the variance was accounted for.

High correlations were shown between snow water equivalent (w.e.) and elevation at five snow courses on Marmot basin (Golding 1969). The snow courses were on a central ridge with similar slope, aspect and forest conditions. Snow w.e. at the 50 points on these snow courses was significantly correlated with forest density (Golding and Harlan 1972). Highly significant correlations were obtained when snow w.e. was correlated with elevation and weighted

stand density (Golding 1970a). For example, for April 1966 the correlation coefficient was 0.91. For the same date the correlation of snow w.e. with elevation alone was 0.81, and with elevation and a single, unweighted measure of stand density, 0.87.

Snow w.e. at maximum pack (approximately March 20) at 200 points on Marmot basin was correlated with 14 combinations of the variables of elevation, slope, aspect, and stand density. Variation accounted for was only 23% (Golding 1970b). It was thought that the model would be improved by including an independent variable to index relative topographic position on the basin.

Runoff and Snow Accumulation

The relationship between runoff and snow accumulation has often been studied to predict runoff for short periods. Garstka *et al.* (1958) related daily snowmelt runoff to temperature, radiation, humidity, wind, and accumulated antecedent runoff. Runoff has also been related to areal extent of snow cover throughout the melt season, e.g., Leaf (1971) in Colorado. The present paper deals with the relationship of runoff during the snowmelt period with maximum snowpack.

3 Method

The first snow courses on Marmot basin were established in 1961 and were intended to provide an *index* of snow accumulation on the basin. The courses consist of ten points, 15–30 m apart. Snow depth and w.e. are measured monthly during the snow season. Based on an analysis of the correlation between snow courses, the twenty courses were reduced to seven in 1969. Data for 1967–1972 for the seven courses are used in this study.

For the four years, 1969–1972, a much more intensive snow sampling program was carried out. Snow depth and w.e. were measured in late March at over 1500 points on a 20.1 m (east-west) × 201.2 m (north-south) grid. Most of the sampling points are below tree line (Fig. 1). At every fifth point east-west the following were recorded:

ELEVATION: in 30.48-m classes above mean sea level; range 1707 m–2315 m.

SLOPE: inclination of the ground surface from the horizontal in 10% classes, representative of an area of about 25 m radius centered on the sample point; range 1–8.

ASPECT: azimuth of slope of ground surface in 45° classes, representative of an area of about 25 m radius centered on the sample point; range 1–8.

FOREST DENSITY: number of trees whose diameters subtend an angle equal to or greater than 147.34 minutes with vertex at the sampling point. This is known as the Bitterlich point-sampling method. Its use in estimating snow w.e. is described by Golding and Harlan (1972). Range 0–34.

On a subsample of 105 consisting of the fifth point on every third east-west line, position relative to local topographic features of the basin was recorded. These were coded as follows:

1. on ridge top

2. in valley bottom
3. on major slope
4. on minor slope
5. on flat or gentle slope

Streamflow is gauged year-round using Stevens A-35 stage recorders with three concrete V-notch weirs and a metal H-type flume on the four main streams of the basin.

4 Results and discussion

Snow Accumulation Models

Multiple regression model. Two snow-accumulation models were constructed using data from 105 sample points measured in 1970 on Marmot basin. Model I consisted of six combinations of four variables that had earlier been shown to be significantly related to snow w.e. (i.e. *FOREST DENSITY*, *SLOPE*³, *ASPECT*², *ELEVATION*², *ELEVATION* × *SLOPE*, *FOREST DENSITY*²), and accounted for 36% of the variation in snow w.e.

Model II consisted of the first and second power of *ELEVATION* and *FOREST DENSITY*, the first, second, and third power of *SLOPE*, *ASPECT*, and *POSITION*, and the interactions of *POSITION* × *ELEVATION*, *POSITION* × *SLOPE*, *ELEVATION* × *SLOPE*, and *POSITION* × *SLOPE* × *ELEVATION*. This model accounted for 51% of the variation. By successive elimination of the variable that contributed least to variance accounted for by the regression equation, the regression was obtained in which all variables were significant at the 95% level of probability. This model accounted for 48% of the variation in snow w.e.:

$$Y = -60.3997 + 83.0575X_1 - 32.7528X_2 + 3.9168X_3 + 0.0674X_4 \\ + 0.7146X_5 - 0.00536X_6 - 0.1137X_7 - 0.3122X_8$$

where Y = snow w.e. (in cm)

$$X_1 = POSITION$$

$$X_2 = POSITION^2$$

$$X_3 = POSITION^3$$

$$X_4 = ELEVATION^2$$

$$X_5 = SLOPE^2$$

$$X_6 = FOREST DENSITY^2$$

$$X_7 = ASPECT^2$$

$$X_8 = ELEVATION \times SLOPE$$

In this model, the partial correlations of snow w.e. on each of the eight independent variables (holding the remaining seven constant) were all significant at the 99% level of probability.

Simple regression model. Regressions were run of each independent variable with grid snow w.e. measured in March of each year. In 1969, for every 100 m increase in elevation, w.e. increased by 1.25 cm. The increase in 1970 was 1.83 cm/100 m elevation rise and in 1971 3.92 cm/100 m. These relationships

TABLE 1. Mean snow w.e. by aspect and topographic position (105 points measured in 1970).

Aspect	Number of samples	Mean snow w.e. (cm)
Southwest	9	6.81
Northwest	4	9.70
South	16	11.46
North	12	12.19
Northeast	15	12.78
East	29	13.56
Southeast	18	14.32
West	2	18.42

Position	Number of samples	Mean snow w.e. (cm)
Ridge top	5	9.40
Gentle slope	5	9.60
Minor slope	10	9.93
Major slope	78	12.50
Valley bottom	7	20.87

will change from year to year, depending on the amount of snowfall. A more useful measure is obtained by weighting the increase with the basin snow w.e. for that year (i.e., by dividing by the mean of the grid points measured in March of that year). The rates for 1970 and 1971 are similar, 0.15 cm and 0.14 cm w.e. increase/100 m elevation rise for each cm of mean snow w.e. The rate for 1969 is only 0.07 cm.

In 1970, southwest and northwest aspects accumulated least snow (6.81 cm and 9.70 cm w.e. respectively), whereas east and southeast accumulated most (13.56 cm and 14.32 cm w.e.), disregarding west aspect for which there were only two samples (Table 1).

Snow w.e. decreased by 1.04 cm/10% slope increase in 1970. This is 0.084 cm/10% slope/cm mean snow w.e. This compares to a decrease of 1.07 cm/10% slope increase in 1969, or 0.064 cm/10% slope/cm mean snow w.e.

As forest density increases, snow w.e. decreases. The measure of forest density is tree count as determined by the Bitterlich point-sampling method. As tree count increased by one, snow w.e. decreased by 0.15 cm in 1969, 0.28 cm in 1970, and 0.43 cm in 1971, with no correlation being evident between the size of decrease and the amount of the annual snow pack.

For position classes, snow w.e. increased from 9.40 cm on ridge tops to 12.50 cm on major slopes to 20.87 in valley bottoms.

Correlation of Snow Course and Grid w.e.

March snow w.e. at each snow course was correlated with mean March w.e. on each of the four areal breakdowns of the basin (Twin, Middle, and Cabin sub-basin, and Marmot basin which includes the three sub-basins and an area below their confluence), giving a sample size of four in each case. March mean w.e.

TABLE 2. Correlation of mean sub-basin snow w.e. with snow course snow w.e. (sample size 4, 1969–1972).

Snow course	Location	Correlation coefficients ¹			
		Marmot basin	Twin sub-basin	Middle sub-basin	Cabin sub-basin
1	Lower confluence	0.96	0.95	0.96	0.95
3	Lower Middle	0.99	0.98	0.98	0.98
6	Confluence	0.96	0.96	0.96	0.96
8	Upper confluence	0.97	0.96	0.96	0.96
11	Middle	0.98	0.97	0.97	0.97
14	Middle	0.99	0.99	0.97	0.99
19	Upper Middle	0.98	0.98	0.98	0.99
Mean	—	0.98	0.98	0.98	0.98

¹Correlation coefficients are significant at the 95% probability level if ≥ 0.95 .

was obtained from the grid sample of 1500 points (Fig. 1). Data for the four years, 1969–1972, was used.

All correlations were significant at the 95 per cent probability level and ranged from 0.95 to 0.99 (Table 2). Although the differences between the coefficients are not significant, snow course 14 gives consistently higher correlations, followed by courses 3 and 19. These three courses are all in Middle sub-basin. Coefficients were highest for the correlations of snow course w.e. with mean Marmot w.e., followed by those with Cabin mean w.e. It would be expected that the best index of mean sub-basin snow accumulation would be a snow course within that basin, but such courses were no better than other courses.

Correlation of Runoff and Snow w.e.

For the correlation of runoff and snow accumulation, two runoff periods were used: snowmelt periods May 1 – June 30 and May 1 – July 31. Snow accumulation was for three measurements: March and maximum pack at the snow courses (five years' data, 1967–1971), and mean sub-basin w.e. from the March grid sampling (four years' data, 1969–1972). Whereas the snow courses provide only an index to basin snow accumulation, the grid sampling provides an estimate of the mean basin snow accumulation. However, much of the streamflow originates from snowmelt in the area above timberline, an area that is essentially unsampled by the grid sampling (Fig. 1). The grid sampling, therefore, becomes only an index to mean snow accumulation of the whole basin.

Highest correlation with snow w.e. was obtained for May 1 – June 30 runoff. Although snowmelt runoff continues into July, the poorer correlation for the period May 1 – July 31 is due to such factors as rainfall and evapotranspiration during the extra month. May 1 – June 30 runoff had higher correlation with March snow-course measurements (median correlation coefficient of 0.89 with 23 of the 32 correlations significant at the 95% level of probability) (Table 3) than with either the maximum snow-course measurement (median

TABLE 3. Correlation of May 1–June 30 runoff with March snow course w.e. (sample size 5, 1967–1971).

Snow course	Correlation coefficients ¹			
	Marmot basin	Twin sub-basin	Middle sub-basin	Cabin sub-basin
1	0.91	0.89	0.94	0.99
3	0.88	0.83	0.94	0.98
6	0.94	0.88	0.96	0.94
8	0.94	0.88	0.94	0.82
11	0.84	0.76	0.89	0.89
14	0.73	0.62	0.76	0.57
19	0.89	0.84	0.93	0.97
Mean	0.94	0.88	0.97	0.89

¹Correlation coefficients are significant at the 95% probability level if ≥ 0.88 .

of 0.81 with 11 of the 32 correlations significant) or the mean snow w.e. (median of 0.84 with none significant). It is surprising that the mean sub-basin snow w.e. did not give the highest correlations in that these values are the average of many point measurements across the sub-basin. There was no trend of runoff being more highly correlated with mean snow w.e. from a particular sub-basin than from any other.

Highest correlations with May – June runoff were obtained with snow course 1 and 6 (Table 3). Both of these courses are in the confluence area of the basin. Those courses that were expected to provide the best indices of snow accumulation on the basin were those that were centrally located. However, these courses, 11, 14, and 19, had the lowest correlation with May – June runoff.

The regression of runoff on the March measurement of snow w.e. at snow course 1, for example, was:

$$Y = 10.24 + 0.71 X$$

where Y = May – June runoff from Cabin Creek, in cm over the sub-basin
 X = snow in March at snow course 1, in cm w.e.

The standard error of estimate of this regression is 0.81 cm of runoff, or 4.3% of the mean May – June runoff from Cabin sub-basin. The value of the intercept, 10.24 cm, represents runoff resulting from precipitation falling during the period April 1 – June 30. This precipitation, made up of both snow and rain, is not included in the March measurement of snow accumulation.

5 Conclusions

Variables having the greatest effect on snow accumulation on Marmot Creek are elevation, topographic position, aspect, slope, and forest density. Of the variation in snow accumulation, 48% is accounted for by a multiple regression model constructed using combinations of these variables.

Snow courses are significantly correlated with an intensive snow survey conducted on the basin and provide an acceptable index of snow accumulation.

May 1 – June 30 streamflow was significantly correlated with March snow course w.e., with standard errors of estimate for the regression being as small as 4.3% of mean streamflow.

References

- ANDERSON, H.W., 1967: Snow accumulation as related to meteorological, topographic, and forest variables in Central Sierra Nevada, California. Pub. No. 78, Int. Assoc. Sci. Hydrology, 215–224.
- FFOLIOTT, P.F., and E.A. HANSEN, 1968: Observations of snowpack accumulation, melt, and runoff on a small Arizona watershed. U.S.D.A. Forest Serv. Res. Note RM-124. 7 pp.
- GARSTKA, W.U., L.D. LOVE, B.C. GOODELL, and F.A. BERTLE, 1958: Factors affecting snowmelt and streamflow. U.S.D.A. Forest Serv. Rocky Mt. Forest and Range Expt. Sta. 189 pp.
- GOLDING, D.L., 1969: Snow relationships on Marmot Creek experimental watershed. Bi-monthly Research Notes, Canada Dept. Fisheries and Forest. Ottawa, 25(2):12–13.
- 1970a: Research results from Marmot Creek experimental watershed, Alberta, Canada. Proc. Symp. On the Results of Research on Representative and Experimental Basins, Wellington, N.Z. Pub. No. 96, Int. Assoc. Sci. Hydrology, 397–403.
- 1970b: Computer mapping of the Marmot Creek snowpack and the influence of topographic and forest-stand variables on the pack. Proc. 3rd Forest Microclimate Symp., Can. Forest. Serv., Alberta/Territories Reg., Calgary, 76–83.
- GOLDING, D.L., and R.L. HARLAN, 1972: Estimating snow-water equivalent from point-density measurements of forest stands. *Ecology*, **53**, 724–725.
- LEAF, C.F., 1971: Areal snow cover and disposition of snowmelt runoff in Central Colorado. U.S.D.A. Forest Serv. Res. Pap. RM-66. 19 pp.
- PACKER, PAUL E., 1962: Elevation, aspect, and cover effects on maximum snowpack water content in a western white pine forest. *Forest Sci.*, **8**, 225–235.
-

BOOK REVIEW

ONE COSMIC INSTANT. John A. Livingston. McClelland and Stewart Limited, Toronto, 1973, 243 pp; \$7.95

"One cosmic instant" is how John Livingston describes what will be the career of the species, man, and the phrase makes an appropriate book title. The book is a scholarly and easy-to-read work dealing with man and his environment. For the purposes of this review, I have summarized what I feel are Livingston's principal observations, hypotheses and conclusions.

The extinction of man is as inevitable as his appearance in the cosmos was contingent. Yet man with his overspecialized brain has been able to rationalize the absence of meaning, purpose and design in the cosmos, explain the mysterious forces which used to awaken his awe and reverence, and create a concept of himself as a species quite different from and above the rest of the biological environment. Intellectually he understands biological symbiosis, but in practice he subdues nature and reserves his admiration for the victories of human technology. He has in fact bound himself symbiotically to his technological world, and it is this egocentricity which has brought the natural world environment to the point of crisis.

The study of evolutionary processes is replete with examples of over-specialization leading relentlessly, sometimes quickly, to extinction; the astonishingly large brain of man is a hyperspecialization that, in its arrogance, will eventually be dealt with. There is no question that reason and intelligence are the most effective instruments that humankind possesses; unfortunately, they very frequently lead him to underestimate his ignorance, and this self-deception will probably be his undoing. As Darwin observed: "Ignorance more frequently begets confidence than does knowledge".

The objective of all species is, of course, survival. In order for man to delay his extinction, he must find the humility to adopt an ethic towards the environment. This is certainly within the realm of the possible because while we cannot change our biological inheritance, we can and do consciously change our cultures. However, the change in this particular case will be difficult because, fundamentally, an environmental ethic runs contrary to our cultural traditions. The evidence suggests that man considered himself apart from nature even before he could consciously articulate the idea.

Livingston points out that ethics have been associated with man-to-man or man-to-society relationships. They have not been concerned with man's relationships to the non-human. As a general observation, we could say that our attitude to the nonhuman world is not immoral, it is amoral.

The achievement of an environmental ethic to guide our behaviour towards the non-human world will require the willingness to see ourselves in the perspective of time of infinite duration and events of unimaginable magnitude. This means that we will have to abandon certain cherished beliefs and reject the negative elements of our traditions; an experience which is likely to be traumatic. We will also have to avoid entertaining the notion that we will redeem nature by technological cleansing because this may well lead to the total destruction of blue earth. We should be aware that nobody is in charge of the technological machine, and that in its mindless acceleration, it may run away with all nature. What it boils down to is that the power structure that culture has created over nature will have to be destroyed.

The power structure, which is characterized by symbiotic interrelationships, acts in a fashion exactly analogous to an ecosystem. The easiest way to destroy an ecosystem is to simplify it. Livingston suggests a number of power structure simplifications which will hasten its demise; for example, removing or subverting man's "rights" to such things as land ownership, having children, raising children, populating at will, killing non-human

species for amusement, dominating other species and the landscape, and so on. We must dismantle the institutions which have kept us locked in with "progress", and develop greater acceptance of communally organized and ordained roles, even though we may not now relish the kinds of society this may entail and may even consider them less "human". Livingston warns that if we do not consciously shift direction and do these things, the environment will do them for us, but in a most agonizing manner.

It has been said that human life has meaning because we create and develop our futures. As humans, we can make projections, and hopefully these will make us recoil, reconsider, and re-create. Our ultimate vision should rest on the vitality of the human will, and on human creativity, enterprise and goodwill. Faith, I think it's called - but it is very hard not to be pessimistic.

The dust jacket of this book observes that once in a long time a book appears that takes a new direction. I would agree that "One Cosmic Instant", as an original and profound study of man's fancied separation from nonhuman nature, is such a work. In my opinion, the book should be on the "must read" list of every meteorologist along with all other thinking members of society.

H.B. Kruger
Atmospheric Environment Service
Toronto

ALBERTA HAILSTORMS

by

A.J. Chisholm (Part I) Marianne English (Part II)

Preface by W.F. Hirschfeld

The essays in this monograph, prepared as a part of the McGill University contribution to the Alberta Hail Studies Project, are concerned with the structure and dynamics of typical hailstorms.

In Part I, Radar Case Studies and Airflow Models, Dr. Chisholm describes and analyzes the radar echo patterns of four hailstorms, and from such analyses, makes deductions pertaining to the inflow, updraft and outflow in such storms and the extent to which the storm structure interacts with and is dependent upon that of the environment.

In Part II, Growth of Large Hail in the Storm, Dr. English marshalls a great deal of knowledge pertaining to hailstones to deduce (in part from Dr. Chisholm's work) simple models of storm updraft from which computations are made of the subsequent growth and trajectories of hailstone embryos.

Meteorological Monographs

Vol. 14, No. 36

November 1973

Send orders to

98 pages

\$8 AMS Members

\$15 Nonmembers

AMERICAN METEOROLOGICAL SOCIETY

45 Beacon Street, Boston, Massachusetts 02108

INFORMATION FOR AUTHORS

Editorial policy. *Atmosphere* is a medium for the publication of the results of original research, survey articles, essays and book reviews in all fields of atmospheric science. It is published quarterly by the CMS with the aid of a grant from the Canadian Government. Articles may be in either English or French. Contributors need not be members of the CMS nor need they be Canadian; foreign contributions are welcomed. All contributions will be subject to a critical review before acceptance. Because of space limitations articles should not exceed 16 printed pages and preferably should be shorter.

Manuscripts should be submitted to: the Editor, *Atmosphere*, West Isle Office Tower, 5th Floor, 2121 Trans-Canada Highway, Dorval, Quebec H9P 1J3. Three copies should be submitted, typewritten with double spacing and wide margins. Heading and sub-headings should be clearly designated. A concise, relevant and substantial abstract is required.

Tables should be prepared on separate sheets, each with concise headings.

Figures should be provided in the form of two copies of an original which should be retained by the author for later revision if required. A list of legends should be typed separately. Labelling should be made in generous size so that characters after reduction are easy to read. Line drawings should be drafted with India ink at least twice the final size on white paper or tracing cloth. Photographs (halftones) should be glossy prints at least twice the final size.

Units. The International System (SI) of metric units is preferred. Units should be abbreviated only if accompanied by numerals, e.g., '10 m', but 'several metres.'

Footnotes to the text should be avoided.

Literature citations should be indicated in the text by author and date. The list of references should be arranged alphabetically by author, and chronologically for each author, if necessary.

RENSEIGNEMENTS POUR LES AUTEURS

Politique éditoriale. *Atmosphère* est un organe de publication de résultats de recherche originale, d'articles sommaires, d'essais et de critiques dans n'importe lequel domaine des sciences de l'atmosphère. Il est publié par la SMC à l'aide d'une subvention accordée par le gouvernement canadien. Les articles peuvent être en anglais ou en français. Il n'est pas nécessaire que les auteurs soient membre de la SMC; les contributions étrangères sont bienvenues. A cause des limitations d'espace les articles ne doivent pas dépasser 16 pages dans le format final. Tout article sera soumis à un critique indépendant avant d'être accepté.

Les manuscrits doivent être envoyés à : le Rédacteur, *Atmosphère*, West Isle Office Tower, 5e étage, 2121 route Trans-canadienne, Dorval, Québec H9P 1J3. Ils doivent être soumis en trois exemplaires dactylographiés à double interlignes avec de larges marges. Les titres et sous-titres doivent être clairement indiqués. Chaque article doit comporter un résumé qui soit concis, pertinent et substantiel.

Les tableaux doivent être préparés et présentés séparément accompagnés d'un titre et d'un numéro explicatifs concis.

Les graphiques doivent être présentés en deux copies dont les originaux devraient être conservés par l'auteur au cas où ils seraient nécessaire de les reviser. Une liste des légendes des graphiques doit être dactylographiée séparément. L'étiquetage doit être de grand format de façon à ce qu'il soit facilement lisible après réduction du format. Le traçage des lignes doit s'effectuer au moyen d'encre de chine en doublant, au moins, le format final, le tout sur papier blanc ou sur papier à calquer et identifié adéquatement. Les photographies (demi-teintes) devraient être présentées sur épreuves glacées au double du format final.

Les unités. Le Système International (SI) d'unités métriques est préférable. Les unités devraient être abrégées seulement lorsqu'elles sont accompagnées de nombres, ex: "10m", mais "plusieurs mètres".

Les notes de renvoi au texte doivent être évitées.

Les citations littéraires doivent être indiquées dans le texte selon l'auteur et la date. La liste des références doit être présentée dans l'ordre alphabétique, par auteur et, si nécessaire, dans l'ordre chronologique pour chaque auteur.

The Canadian Meteorological Society / La Société Météorologique du Canada

The Canadian Meteorological Society came into being on January 1, 1967, replacing the Canadian Branch of the Royal Meteorological Society, which had been established in 1940. The Society exists for the advancement of Meteorology, and membership is open to persons and organizations having an interest in Meteorology. At nine local centres of the Society, meetings are held on subjects of meteorological interest. *Atmosphère* as the scientific journal of the CMS is distributed free to all members. Each spring an annual congress is convened to serve as the National Meteorological Congress.

Correspondence regarding Society affairs should be directed to the Corresponding Secretary, Canadian Meteorological Society, P.O. Box 160, Ste-Anne-de-Bellevue, P.Q. H9X 3L5

There are three types of membership - Member, Student Member and Sustaining Member. For 1974 the dues are \$15.00, \$5.00 and \$50.00 (min.), respectively. The annual Institutional subscription rate for *Atmosphère* is \$10.00.

Correspondence relating to CMS membership or to institutional subscriptions should be directed to the University of Toronto Press, Journals Department, 5201 Dufferin St., Downsview, Ontario, Canada, M3H 5T8. Cheques should be made payable to the University of Toronto Press.

La Société météorologique du Canada a été fondée le 1^{er} janvier 1967, en remplacement de la Division canadienne de la Société royale de météorologie, établie en 1940. Cette société existe pour le progrès de la météorologie et toute personne ou organisation qui s'intéresse à la météorologie peut en faire partie. Aux neuf centres locaux de la Société, on peut y faire des conférences sur divers sujets d'intérêt météorologique. *Atmosphère*, la revue scientifique de la SMC, est distribuée gratuitement à tous les membres. À chaque printemps, la Société organise un congrès qui sert de Congrès national de météorologie.

Toute correspondance concernant les activités de la Société devrait être adressée au Secrétaire-correspondant, Société météorologique du Canada, C.P. 160, Ste-Anne-de-Bellevue, P.Q. H9X 3L5

Il y a trois types de membres: Membre, Membre-étudiant, et Membre de soutien. La cotisation est, pour 1974, de \$15.00, \$5.00 et \$50.00 (min.) respectivement. Les Institutions peuvent souscrire à *Atmosphère* au coût de \$10.00 par année.

La correspondance concernant les souscriptions au SMC ou les souscriptions des institutions doit être envoyée aux Presses de l'Université de Toronto, Département des périodiques, 5201 Dufferin St., Downsview, Ontario, Canada, M3H 5T8. Les chèques doivent être payables aux Presses de l'Université de Toronto.

Council/Conseil d'Administration: 1973-74

<i>President/Président</i>	- W.F. Hitschfeld	<i>Councillors-at-large/ Conseillers</i>
<i>Vice-President/Vice-Président</i>	- A.J. Robert	A.F. McQuarrie
<i>Past President/Président sortant</i>	- G.A. McKay	R.H. Silversides
<i>Corresponding Secretary/ Secrétaire-correspondant</i>	- F.J. Lemire	C.V. Wilson
<i>Treasurer/Trésorier</i>	- I.N. Yacowar	<i>Chairmen of Local Centres/ Présidents des centres</i>
<i>Recording Secretary/ Secrétaire d'assemblée</i>	- J.F. Derome	

ATMOSPHERE

<i>Editorial Committee/Comité de rédaction</i>		
<i>Editor/Rédacteur</i>	I.D. Rutherford	
<i>Associate Editors/ Rédacteurs Associés</i>	C. East	D.N. McMullen
	J.B. Gregory	P.E. Merilees
	W. Gutzman	R.R. Rogers
	R. List	V.R. Turner
	C.L. Mateer	E.J. Truhlar
	G.A. McBean	E. Vowinkel

Sustaining Member/Membre de soutien

Air Canada